ORNL/CON-50

ornl

OAK
RIDGE
NATIONAL
LABORATORY

UNION
CARBIDE

Ice-Maker Heat Pump Development: Final Report

Van D. Baxter

OPERATED BY
UNION CARBIDE CORPORATION
FOR THE UNITED STATES
DEPARTMENT OF ENERGY

Printed in the United States of America. Available from
National Technical Information Service
U.S. Department of Commerce
5285 Port Royal Road, Springfield, Virginia 22161
NTIS price codes—Printed Copy: A05 Microfiche A01

This report was prepared as an account of work sponsored by an agency of the United States Government. Neither the United States Government nor any agency thereof, nor any of their employees, makes any warranty, express or implied, or assumes any legal liability or responsibility for the accuracy, completeness, or usefulness of any information, apparatus, product, or process disclosed, or represents that its use would not infringe privately owned rights. Reference herein to any specific commercial product, process, or service by trade name, trademark, manufacturer, or otherwise, does not necessarily constitute or imply its endorsement, recommendation, or favoring by the United States Government or any agency thereof. The views and opinions of authors expressed herein do not necessarily state or reflect those of the United States Government or any agency thereof.

ORNL/CON-50

Contract No. W-7405-eng-26

Energy Division

ICE-MAKER HEAT PUMP DEVELOPMENT: FINAL REPORT

Van D. Baxter

Department of Energy
Division of Buildings and Community Systems

Date Published: September 1980

OAK RIDGE NATIONAL LABORATORY
Oak Ridge, Tennessee 37830
operated by
UNION CARBIDE CORPORATION
for the
DEPARTMENT OF ENERGY

RELATED REPORTS IN THIS SERIES

1. H. C. Fischer et al., *Summary of Annual Cycle Energy System Workshop I*, held Oct. 29–30, 1975, Oak Ridge, Tenn., ORNL/TM-5243, Oak Ridge National Laboratory, Oak Ridge, Tenn., July 1976.
2. J. C. Moyers et al., *Design Report for the ACES Demonstration House*, ORNL/CON-1, Oak Ridge National Laboratory, Oak Ridge, Tenn., October 1976.
3. E. A. Nephew et al., *The Annual Cycle Energy System: Initial Investigations*, ORNL/TM-5525, Oak Ridge National Laboratory, Oak Ridge, Tenn., October 1976.
4. I. G. Cantor, *Investigation of Alternate Types of Water Storage Components to be Utilized in Conjunction with the ACES System*, ORNL/Sub-78/14233/1, Oak Ridge National Laboratory, Oak Ridge, Tenn., December 1977.
5. E. C. Hise, *Performance Report for the ACES Demonstration House, August 1976 through August 1977*, ORNL/CON-19, Oak Ridge National Laboratory, Oak Ridge, Tenn., March 1978.
6. H. C. Fischer, *Development and Testing of a Single-Plate and a Two-Plate Ice-Maker Heat Pump*, ORNL/CON-21, Oak Ridge National Laboratory, Oak Ridge, Tenn., April 1978.
7. A. S. Holman and V. R. Brantley, *ACES Demonstration: Construction, Startup, and Performance Report*, ORNL/CON-26, Oak Ridge National Laboratory, Oak Ridge, Tenn., October 1978.
8. V. D. Baxter, *Intermediate Report on the Performance of Plate-Type Ice-Maker Heat Pumps*, ORNL/CON-23, Oak Ridge National Laboratory, Oak Ridge, Tenn., October 1978.
9. A. S. Holman et al., *Annual Cycle Energy System (ACES) Performance Report, November 1977 through September 1978*, ORNL/CON-42, Oak Ridge National Laboratory, Oak Ridge, Tenn., May 1980.
10. R. E. Minturn et al., *ACES 1979: Capabilities and Potential*, ORNL/CON-48, Oak Ridge National Laboratory, Oak Ridge, Tenn., May 1980.
11. J. W. MacArthur, *Economic Analysis of Annual Cycle Energy Systems*, ORNL/Sub-7470/V1,V2,V3, Energy Resources Center, Honeywell Inc., Fort Washington, Pa.
12. E. A. Nephew, L. Abbatiello, and M. L. Ballou, *Theory and Design Manual*, ORNL/CON-43, Oak Ridge National Laboratory, Oak Ridge, Tenn., May 1980.
13. M. L. Ballou et al., *MAD: A Computer Program for ACES Design Using Monthly Thermal Loads*, ORNL/CON-51, Oak Ridge National Laboratory, Oak Ridge, Tenn. (in preparation).
14. V. D. Baxter et al., *Final ACES Performance Report, September 1978 through September 1980*, Oak Ridge National Laboratory, Oak Ridge, Tenn. (in preparation).
15. L. A. Abbatiello et al., *Performance and Economics of the ACES and Alternative Residential Heating and Air Conditioning Systems in 115 U.S. Cities*, ORNL/CON-52, Oak Ridge National Laboratory, Oak Ridge, Tenn. (in preparation).

CONTENTS

LIST OF FIGURES v

LIST OF TABLES vii

ACKNOWLEDGMENTS ix

ABSTRACT 1

1. INTRODUCTION 1

2. SUMMARY 3
   2.1 Harvesting Scheme 3
      2.1.1 Hot-gas scheme 3
      2.1.2 Stored-refrigerant scheme 3
      2.1.3 Dual-fluid schemes 4
   2.2 Plate Loading 4
   2.3 Cyclic Losses 4
   2.4 Ice-Packing Density 5

3. DESCRIPTION OF HARVESTING SCHEMES 7
   3.1 Hot-Gas Harvest 7
   3.2 Direct-Subcooling Harvest 7
   3.3 Stored-Energy Schemes 8
      3.3.1 Stored-refrigerant harvest 8
      3.3.2 Dual-fluid harvest 8

4. TEST UNIT DESCRIPTIONS 11
   4.1 Test Unit One 11
   4.2 Test Unit Two 11
   4.3 Test Unit Three 16
   4.4 Test Unit Four 16

5. SYSTEM TESTS 23
   5.1 Harvesting Scheme Evaluations 23
      5.1.1 Hot-gas harvest 24
      5.1.2 Stored-refrigerant harvest 25

5.1.3 Dual-fluid schemes 25
5.2 Plate-Loading Evaluations 26
5.3 System Performance Tests 27
5.3.1 Water-chilling tests 27
5.3.2 Ice-making tests 28
5.3.3 Cyclic tests 31

6. ICE-PACKING DENSITY 35
6.1 Test Procedure 35
6.2 Test Results 36
6.2.1 Brine chiller 36
6.2.2 Plate-type IMHP 36
6.3 Ethylene Glycol Treatment Results 38
6.4 Survey Results 41

7. CONCLUSIONS 43

REFERENCES 45

APPENDIX A—TABULATED TEST RESULTS 47

APPENDIX B—SAMPLE CALCULATIONS 53

APPENDIX C—RELATIONSHIP BETWEEN THE PACKING FACTOR AND THE WEIGHT FRACTION PACKING FACTOR 63

LIST OF FIGURES

Page

Fig. 1. Hot-gas harvesting operation 7

Fig. 2. Dual-series evaporator heat pump with direct-subcooling harvest; evaporator one harvesting 8

Fig. 3. Flow schematic of stored-refrigerant harvesting scheme 9

Fig. 4. Dual-fluid harvesting schematic 9

Fig. 5. Unit one schematic diagram 11

Fig. 6. Test unit one 12

Fig. 7. Unit one schematic diagram; modified hot-gas harvesting scheme 13

Fig. 8. Unit two schematic diagram 14

Fig. 9. Test unit two 15

Fig. 10. Unit three schematic diagram 17

Fig. 11. Test unit three 18

Fig. 12. Section of freezing plate from unit three showing details of harvest and refrigerant circuit manifolding 19

Fig. 13. Freezing plate from unit three 19

Fig. 14. Unit four schematic diagram 20

Fig. 15. Test unit four 21

Fig. 16. Average COP, heating capacity, and harvesting time of unit one vs freeze cycle time for two ambient air temperatures 23

Fig. 17. Section of freezing plate on unit three showing relative location of water distributors 26

Fig. 18. Plate-loading test results on unit two with variable-speed open compressor 27

Fig. 19. Unit one average COP and evaporator temperature difference vs evaporator plate loading 28

Fig. 20. Average evaporating temperature and COP vs tank-water temperature for units one and four 29

Fig. 21. Average suction pressure and COP vs tank-water temperature for units two and three 29

Fig. 22. Average COP vs freeze-cycle length for various IMHP test units 30

Fig. 23. Average COP, heating capacity, and suction pressure vs freeze time 31

Fig. 24. Average COP and heating capacity of unit three as a function of air temperature and freeze-cycle length 32

Fig. 25. Cyclic performance of units two, three, and four as a function of part load and on time 33

Fig. 26. Test unit three harvesting ice 38

Fig. 27. Ice mound produced by IMHP during bulk-sampling test 39

Fig. 28. Cross section showing typical IMHP ice geometry 40

Fig. B.1. Sample test data, refrigerant temperatures, and compressor power vs time 55

Fig. B.2. Sample test data, brine and coolant temperatures, and harvesting pump power vs time 56

Fig. B.3. Cross section of unit two ice tank; measurements taken during bulk-sampling tests are shown 60

LIST OF TABLES

Page

Table 1. Harvest times for units one, three, and four 23

Table 2. Cyclic performance of test units three and four 33

Table 3. Maximum packing factors achieved in ACES house ice bin 37

Table 4. Bucket-sampling test results 37

Table 5. Bulk-sampling test results 37

Table 6. Effect of ethylene glycol on bucket-sample packing factors 40

Table 7. Effect of ethylene glycol on bulk-sample packing factors 40

Table 8. Geometric effects on ice-packing factors 41

Table A.1. Performance of unit one with modified hot-gas harvesting scheme 49

Table A.2. Plate-loading test results using variable-speed open compressor on unit two 49

Table A.3. Variable plate-loading test results for unit one 49

Table A.4. Water-chilling performance of units one and four 50

Table A.5. Water-chilling performance of units two and three 50

Table A.6. Performance of test units in freeze-harvest cycle mode for various freeze cycle lengths 51

Table A.7. Performance of test units under steady freeze (no-harvest) conditions 52

Table B.1. Sample data output for 45-min freeze-cycle test on unit three for period of operation immediately preceding, during, and immediately following an ice-harvesting operation 55

ACKNOWLEDGMENTS

The author thanks P. W. Childs for his extremely important contributions to the collection and analysis of test data and J. T. Farmer for maintenance of the refrigeration equipment. Thanks are also expressed to E. C. Hise and J. C. Moyers for their early guidance and support and to L. A. Abbatiello for his continuing support.

ABSTRACT

Four test unit ice-maker heat pumps (IMHPs) were tested under the Annual Cycle Energy System (ACES) program. Performance results on the effects of harvesting scheme, plate loading, and cycling operation were compared. The ice-packing density of IMHPs was also studied and compared with that of ice manufactured by commercial ice makers and brine-chiller ACES.

Three harvesting schemes were tested: hot-gas, stored-refrigerant, and dual-fluid, off-cycle. The hot-gas scheme tended to penalize excessively the heating output of the system. Stored-refrigerant schemes eliminated that problem but caused compressor failures due to floodback and oil dilution. The dual-fluid schemes exhibited no such problems and demonstrated an ability to harvest during compressor off cycles. Therefore, it was concluded that dual-fluid, off-cycle schemes are the best for use with IMHPs.

Plate-loading tests in which compressor speed and evaporator size are varied clearly showed that evaporator plate loading should be as low as possible.

Cyclic testing showed that cyclic performance can be improved by using nonequalizing refrigerant systems.

Ice-packing density measurements indicated a maximum packing factor for IMHP ice of 0.4 compared with 0.8 for brine-chiller systems. Distributing the ice evenly in water gave better packing factors than did allowing it to pile up under the plates. A survey of commercial ice makers indicated that IMHPs producing cylindrical and cubical ice rather than sheets of ice would have packing factors of 0.8 to 0.66 and thus obvious economic benefits. However, the cost of evaporators for making such ice is not likely to be economical.

1. INTRODUCTION

The increasing cost of energy has increased the effort to determine ways to use energy more efficiently, particularly for space heating and cooling. One of the most effective ways to conserve energy in this area is the Annual Cycle Energy System (ACES),[1,2] a highly efficient heating and cooling system usable in residential and light commercial buildings. Basically a heat pump with low-side storage, the ACES extracts heat from storage (a tank filled with water) to meet building heating and hot water requirements. The ice produced as a by-product is used to meet all or part of the building's cooling requirements.

The ACES forms ice by one of two primary means. One means is a brine-chiller, brine-to-brine heat pump package employing a heat exchanger submerged in the storage tank, such as is used in the ACES demonstration house.[3,4] The other means is a plate-type ice-maker heat pump (IMHP), which was developed as an alternative to the brine-chiller-type mechanical package in an effort to reduce system first cost. An IMHP eliminates the heat exchanger in the storage tank. Ice is formed on refrigerated plates; when these plates are periodically defrosted, ice falls into the bin and floats on the surface of the water.[5,6] This ice, however, doesn't pack as densely as does that formed by the brine-chiller system, which necessitates a larger storage volume. Thus, an economic trade-off exists between the in-bin heat exchanger with its more densely packed ice and the IMHP with its larger bin. This report deals primarily with the IMHP.

Two of the goals in the IMHP development effort have been the ice-harvesting scheme development and an improvement in ice-packing density. This report describes several candidate harvesting schemes and their effects on system performance and reliability. The results of ice-packing studies are also presented.

The ice-harvesting schemes discussed are the hot-gas, stored-refrigerant, and dual-fluid, off-cycle methods. The hot-gas scheme[5] uses the output of the compressor directly for harvesting; the stored-refrigerant and dual-fluid schemes use the heat contained in the liquid refrigerant as it exits the condenser. In the stored-refrigerant system, the liquid refrigerant is used directly by flashing it to a vapor, which is sent to the evaporator; in the evaporator, the vapor condenses and causes the ice to fall into the bin.[5,6] Dual-fluid systems subcool the condensed refrigerant and store the heat in a

secondary fluid until it is needed for harvesting, which can be done through a heat pipe arrangement or by pumping the warm fluid through parallel circuits in the evaporator plates.

Test results reported here show the effects of different harvesting schemes on the performance and reliability of IMHPs. The different harvesting schemes are evaluated to identify the best scheme for use with IMHP systems. Also discussed are the effects on system performance of evaporator plate loading, cyclic operation, reduced air temperature around the plates, and system modifications to improve the harvesting scheme.

Ice-packing density is an important parameter because it determines how large a storage volume will be needed to obtain a desired energy storage capacity. Obviously, the greater the packing density, the smaller (and less expensive) the storage volume required. In this report, the effects of ice geometry and chemical modification of the water on packing density are discussed.

2. SUMMARY

2.1 Harvesting Scheme

2.1.1. Hot-Gas Scheme

The initial test unit, equipped with a hot-gas harvesting system, experienced severe performance penalties because the full output of the compressor was required during the harvesting period. For short freeze times, 10 to 30 min, the COP[a] ranged from 2.2 to 2.7. Modifications made to improve the heat pump's harvesting scheme resulted in increasing the COP range to 2.7 to 3.1 for freeze times of 10 to 70 min; the maximum COP occurred during the 70-min freeze cycle. Improvement was mainly due to reduced interruption of heating operation for harvesting purposes.

System performance deteriorated badly when the plates were enclosed in an insulated box. Harvest times nearly doubled and capacity decreased, indicating the inadvisability of using a hot-gas scheme when operating the plates in a cold environment. Performance also suffered if the hot-gas line between the compressor and the plates was uninsulated or if the line was very long.

Test results show that hot-gas harvesting schemes work efficiently only if the compressor is in close proximity to the plates, if the line between is heavily insulated, and if the plates are located in a relatively warm environment. The adverse effect of these schemes on system performance and heating capacity makes them undesirable for use with IMHPs.

2.1.2 Stored-Refrigerant Scheme

The liquid-refrigerant storage harvesting scheme used on the second test unit operated very efficiently: harvesting was accomplished in 35 s or less and did not seriously affect the heating output of the unit.

Because the energy for harvesting was stored in the liquid refrigerant exiting the condenser, an extra-large refrigerant charge was required to store a sufficient amount of energy for that purpose. This extra charge (about 7.3 to 9.1 kg) seriously jeopardized reliability. During each harvesting cycle, a portion of the stored refrigerant was condensed in the harvesting plate and ended up in the suction-line accumulator or the compressor shell. On start-ups, the liquid remaining in the accumulator was drawn, in a massive slug, into the compressor. This liquid floodback caused the compressor to fail after about one year of operation. Frequent problems with leaky refrigerant control valves resulted in insufficient liquid being available to ensure reliable harvesting. This leakage further complicated compressor lubrication problems. The refrigerant circuit required was complex: many extra valves and fittings were necessary for harvesting control. This caused extra pressure drops and penalized overall system performance.

Although the stored-refrigerant scheme has some advantages over the hot-gas scheme, its tendency to cause liquid floodback to the compressor raises serious doubts about the service life of an IMHP employing this scheme. Better compressor protection techniques and refrigeration circuit designs for effective control of both refrigerant and oil are needed before the stored-refrigerant scheme can be considered a viable option.

---

[a]Refers to the average compressor-only heating COP, that is, the heating output of the heat pump divided by the compressor power input:

$$\text{COP} = \frac{\text{average heat output}}{\text{average compressor power input}}$$

2.1.3. Dual-Fluid Schemes

The two dual-fluid schemes tested exhibited the desirable characteristic of excellent performance over wide ranges of freeze times. Both schemes stored harvesting energy in a secondary fluid by subcooling the liquid refrigerant exiting the condenser. Two different harvesting techniques were employed. One scheme used evaporator plates having seven parallel flow channels; warm harvesting fluid was pumped through four of these channels when necessary. The second scheme used a heat pipe circuit; when harvesting was needed, solenoid valves isolated the evaporator from the rest of the heat pump circuit and connected it to a harvesting coil submerged in the secondary fluid. Liquid refrigerant was drained from the evaporator, vaporized in the harvest coil, and recondensed in the evaporator until harvesting was completed.

The third test unit, equipped with the dual-circuit-plate, pumped harvesting scheme, yielded COPs of 3.00 to 3.20 for freeze times of 1 h to 15 min. Harvesting generally took from less than 2 min (for plates surrounded by 23.9°C air) to as much as 4 min (for plates surrounded by 1.7°C air). Less than 1% of the power used by the unit was needed to operate the harvest pump.

The fourth test unit, equipped with the heat-pipe harvesting scheme, generated similar COPs for freeze times of 10 to 90 min. This scheme generally took about twice as long to harvest the ice as did the pumped system; however, it used no additional electrical power. Since both schemes operated during compressor off cycles, heat pump heating operation was uninterrupted and thus not penalized by the harvesting operation.

These two test units had the advantage of having much simpler refrigeration circuits than those required by the other two schemes. The number of solenoid valves in the circuit was reduced from eight or ten to only two for unit four and one for unit three. In addition, no excessive refrigerant charge was required, thus reducing the possibilities of liquid floodback to the compressor. It is evident that systems using a secondary fluid to store energy for harvesting offer the best defrosting performance and the least adverse affect on IMHP performance and reliability. Accordingly, harvesting systems of this type are recommended for use with IMHPs in future applications, and the pumped harvesting technique is recommended because of its shorter harvesting time.

2.2 Plate Loading

Performance tests show conclusively that the lower the evaporator-plate-loading factor (i.e., the more evaporator area available for a given compressor), the higher the evaporating temperature and COP. Test results indicate that halving the plate loading can result in as much as a 50% increase in COP. Combining low plate loading with harvesting schemes that do not penalize the heating performance of the unit, as in units three and four, results in high levels of performance independent of freeze cycle length. This leads to the conclusion that IMHP evaporators should be as large as is feasible. It is recommended that evaporator-plate-loading factors during the ice-making mode be limited to about 1400 W/m^2.

2.3 Cyclic Losses

Comparison of the cyclic performance of two systems having nonequalizing refrigerant circuits with that of an equalizing system indicates that significant cyclic performance improvements can be attained through the use of a liquid-line solenoid valve to maintain the refrigerant pressure differential during off periods. Generally, it was determined that, for partial loads in excess of about 20% of full load, the nonequalizing systems experienced essentially no degradation of steady-state, full-load performance levels.

2.4 Ice-Packing Density

Ice-packing tests on IMHP plate ice show that a maximum packing factor of about 0.40 is attainable as opposed to 0.80 for the in-bin heat exchanger system. Tests indicate the advisability of distributing IMHP ice evenly in the storage bin rather than allowing it to pile up, which would further reduce the packing factor and hinder harvesting if the pile reached the evaporator plates.

Packing factors could be improved from 0.40 to 0.58 or 0.66 by producing solid cylinders or cubes of ice rather than corrugated sheets. This offers the possible economic advantage of smaller storage bins. The extra cost of evaporators required to make such ice, however, are likely to offset any economic gain of the better packing factor.

3. DESCRIPTION OF HARVESTING SCHEMES

The basic aim of the IMHP harvesting scheme is to remove the ice that accumulates on the evaporator and to deposit it in a storage bin. This function can be accomplished either mechanically or thermally. However, the latter method is recommended because thermal harvesting can be done with little waste of useful energy and because such systems are mechanically less complex. Thermal energy can be delivered directly to the evaporator from the compressor discharge gas or direct subcooling of hot liquid, or it can be stored in some medium and delivered as needed.

3.1 Hot-Gas Harvest

Hot-gas harvesting schemes use compressor discharge gas directly to supply needed heat. Figure 1 illustrates the principle of hot-gas harvesting. In normal operation, the hot refrigerant gas goes from compressor to condenser, through an expansion device to the evaporator, and back to the compressor. When harvesting is needed, the discharge gas valve directs the hot gas around the condenser to the evaporator, where it condenses to harvest the ice. The condensed refrigerant liquid is collected in an accumulator and boiled off during the next freeze cycle.

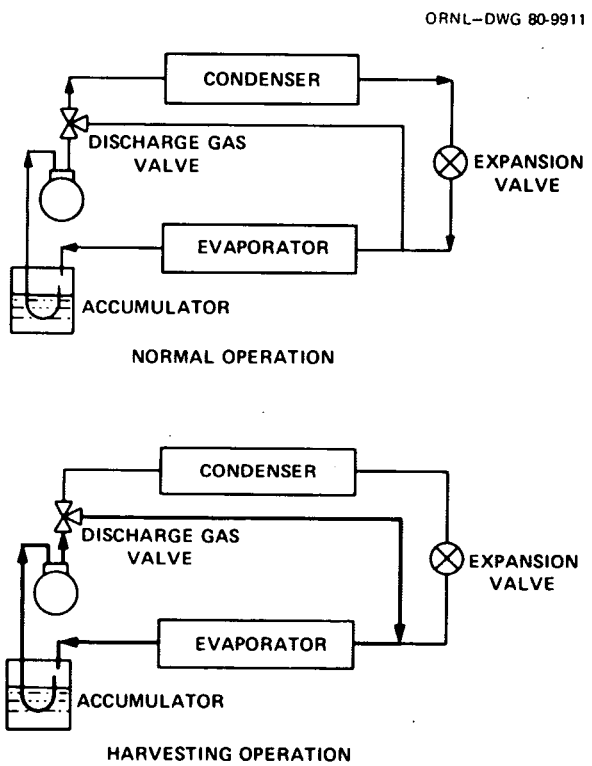

Fig. 1. Hot-gas harvesting operation.

3.2 Direct-Subcooling Harvest

The direct-subcooling scheme is used for harvesting with the dual-series evaporator heat pump described in detail by Mondry.[7] Figure 2 illustrates this scheme.

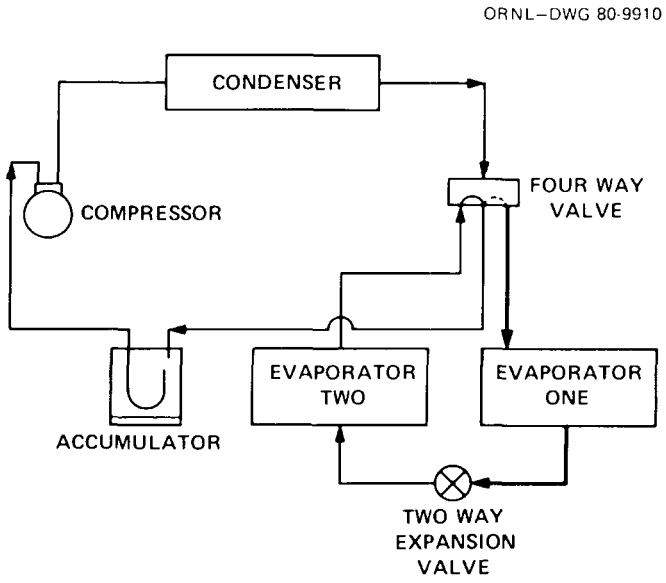

Fig. 2. Dual-series evaporator heat pump with direct-subcooling harvest; evaporator one harvesting.

In normal operation, one of the evaporators is in the harvesting mode at all times. When the active (ice-making) evaporator requires defrosting, the four-way valve switches, and the active evaporator becomes the subcooling (harvesting) evaporator and vice versa. Harvesting is then effected by subcooling the liquid refrigerant from the condenser in the ice-covered evaporator. Reference 7 contains a more detailed discussion of this scheme.

3.3 Stored-Energy Schemes

The two energy storage harvesting schemes discussed in this report are stored refrigerant and storage in a secondary fluid.

3.3.1 Stored-Refrigerant Harvesting

Figure 3 illustrates the stored-refrigerant harvesting scheme. In normal operation, the refrigerant circulates as indicated by the solid arrows. Harvesting energy is stored at the condensing temperature in liquid refrigerant that collects in receiver 2. When harvesting is needed, solenoid valves 1 and 3 close, valve 2 opens, and the refrigerant flows as indicated by the dashed arrows. High-pressure, high-temperature liquid in receiver 2 begins to flash immediately to a warm vapor, which is transferred to the evaporator; in the evaporator the vapor condenses and causes the ice to melt free. Condensed liquid is captured by the accumulator and boiled off during the next freeze cycle. Liquid from the condenser is stored in receiver 1 during harvesting.

An extra-large refrigerant inventory is required to store the needed harvesting energy.

3.3.2 Dual-Fluid Harvesting

In the dual-fluid scheme (Fig. 4), the refrigerant flow path is never altered. Instead, heat is transferred from the liquid refrigerant exiting the condenser to a secondary fluid and is stored in the secondary fluid reservoir until needed. When harvesting is necessary, the compressor is stopped, and

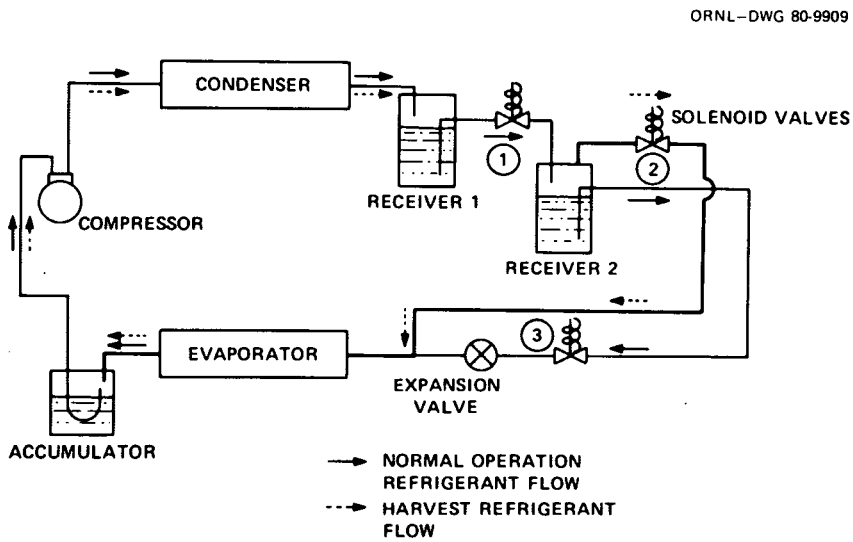

Fig. 3. Flow schematic of stored-refrigerant harvesting scheme.

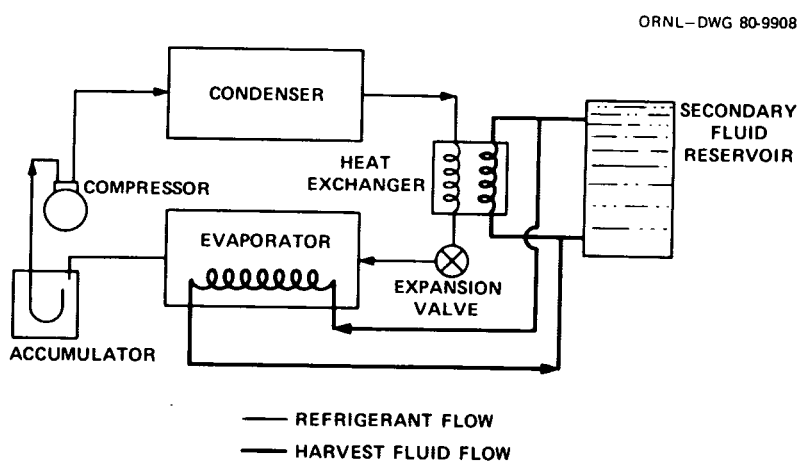

Fig. 4. Dual-fluid harvesting schematic.

the stored energy is transferred to the evaporator. This transfer can be accomplished either by pumping the fluid directly through parallel paths in the heat exchanger or by using a heat pipe arrangement.

4. TEST UNIT DESCRIPTIONS

4.1 Test Unit One

The original configuration of test unit one, the Remcor unit (described in ref. 5), is shown schematically in Fig. 5; Fig. 6 is a photograph of the unit. Harvesting was accomplished by diverting the compressor discharge gas directly to the evaporator plates, one at a time. Total harvest-cycle time was set at 3.5 min, and freeze-cycle duration varied from 10 to 70 min.

After being tested in the original configuration, test unit one was modified to admit the hot gas to the top of the evaporator plates rather than to the bottom. In addition, the size of the R-22 distributor was increased from a 9.5- to a 38-mm OD to drain the condensed refrigerant from the plates more rapidly. This modification is shown in Fig. 7. With the exception of the reversed hot-gas entry and exit points, harvesting was done in essentially the same manner as in the original. Harvest-cycle times were shortened to 2.7 min.

The evaporator of unit one consisted of four copper plates having a total active area of 3.51 m^2. The heating capacity of the unit was about 5900 W at a 41°C condensing temperature and a −5°C evaporating temperature. The refrigerant circuit was nonequalizing; that is, solenoid valves in the liquid line maintained the pressure differential during off periods.

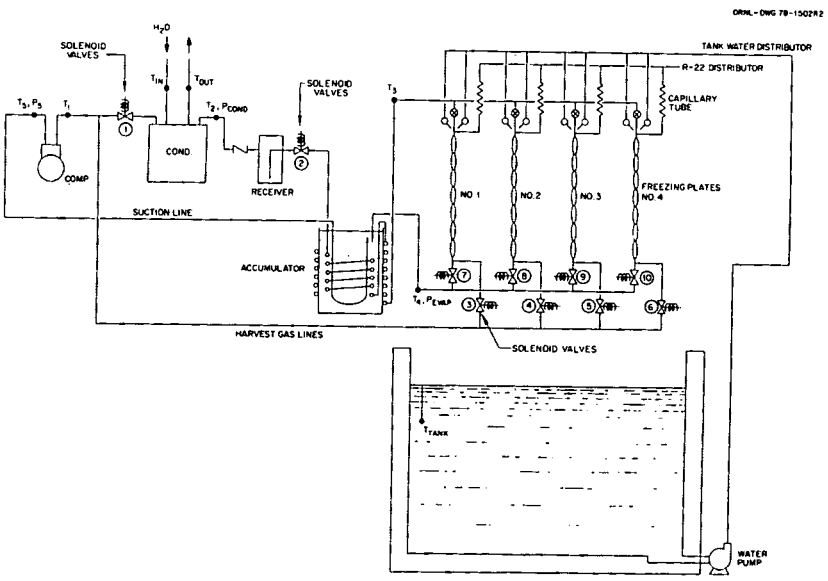

Fig. 5. Unit one schematic diagram.

4.2 Test Unit Two

Unit two, the two-plate IMHP described by Fischer,[6] is shown schematically in Fig. 8, and the photograph in Fig. 9 illustrates the system components. This unit employed the stored-refrigerant method of harvesting. To harvest the ice, valves 1 and 2 and one of the suction-line solenoid valves, 3, closed. Harvesting valve 4, connecting the plate to be harvested with the gas space at the top of receiver 2, opened. Flash boiling of the liquid in receiver 2 forced warm vapor into the top of the

ORNL-PHOTO 6158-77

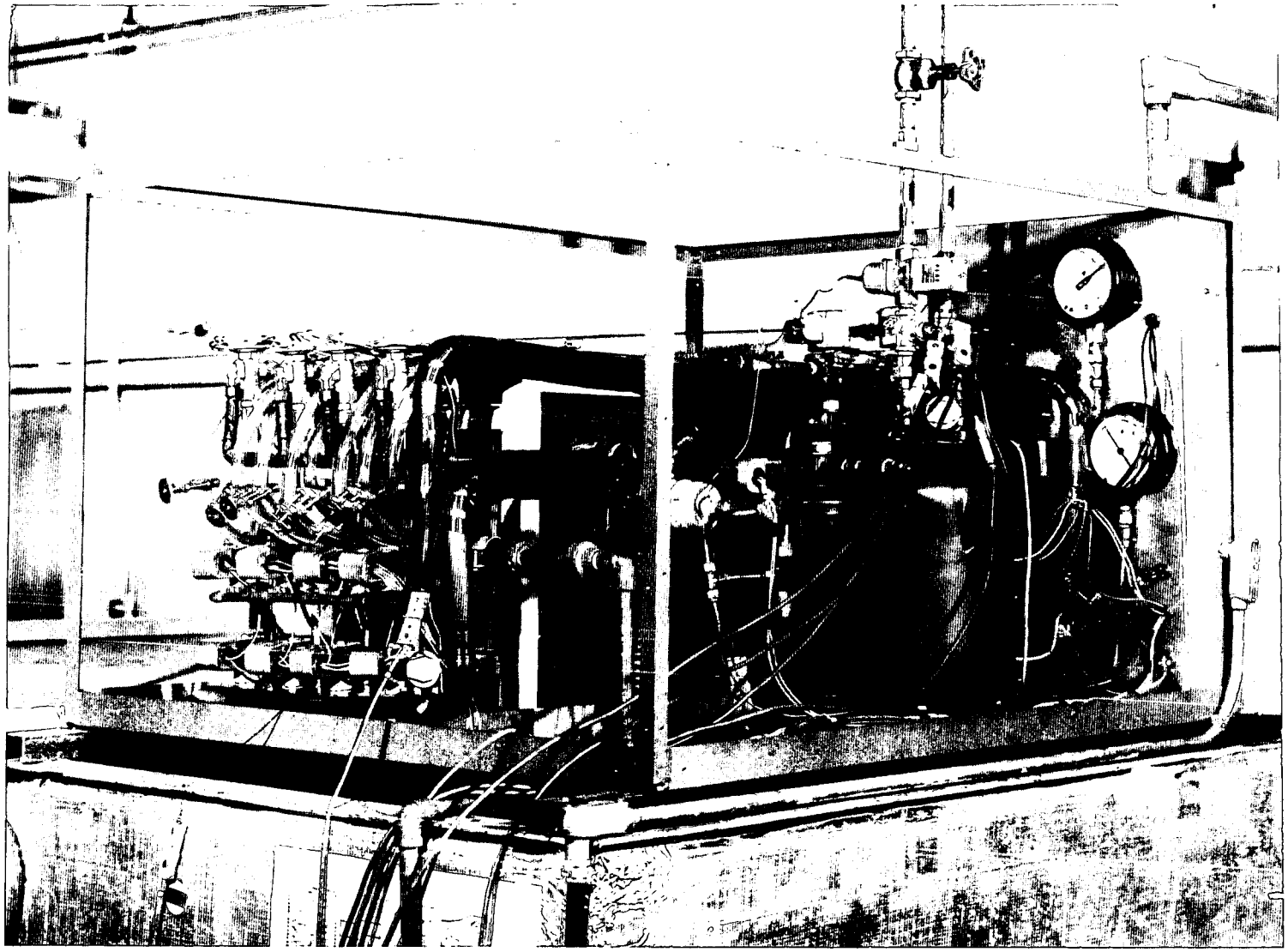

Fig. 6. Test unit one.

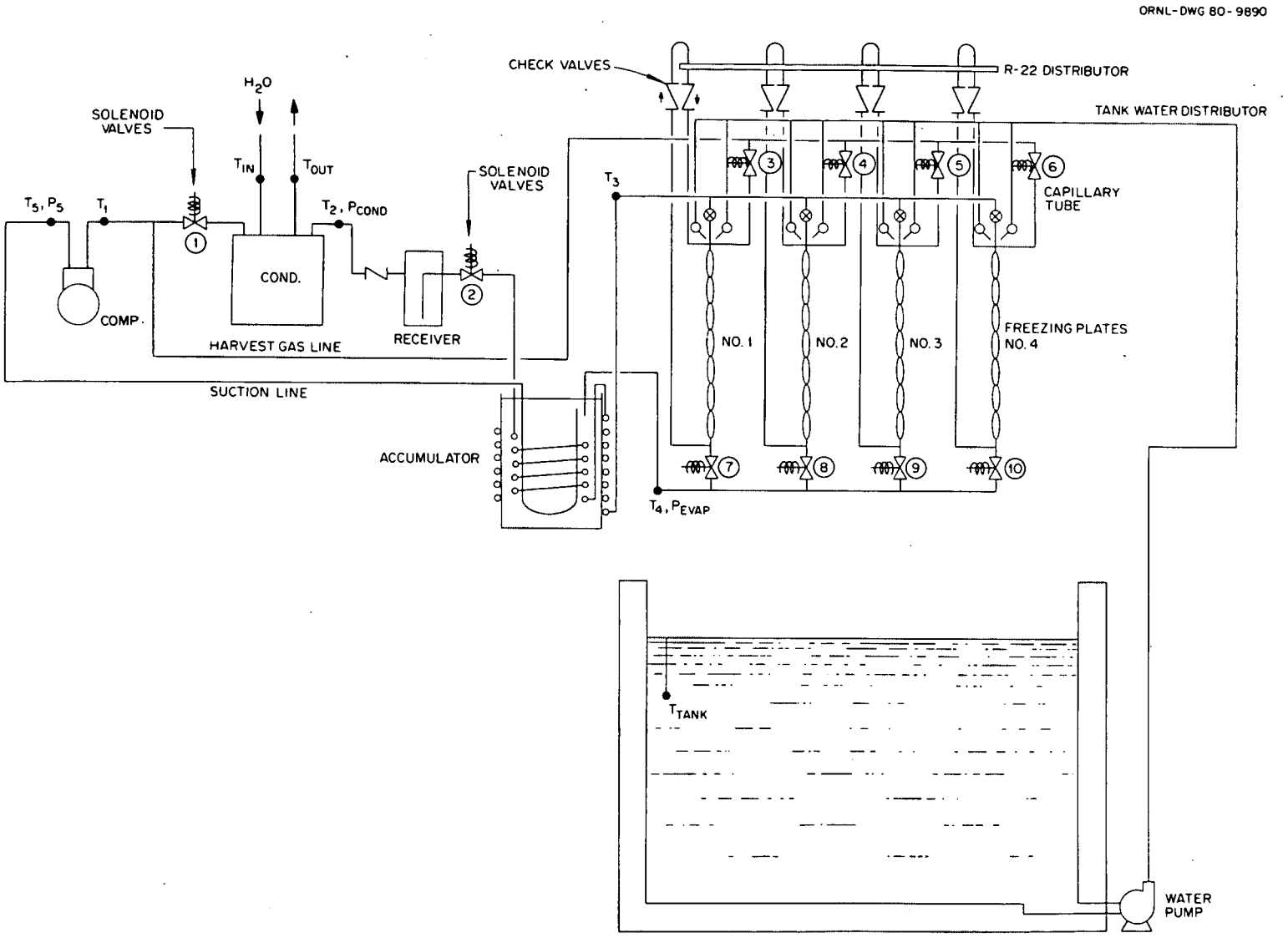

Fig. 7. Unit one schematic diagram; modified hot-gas harvesting scheme.

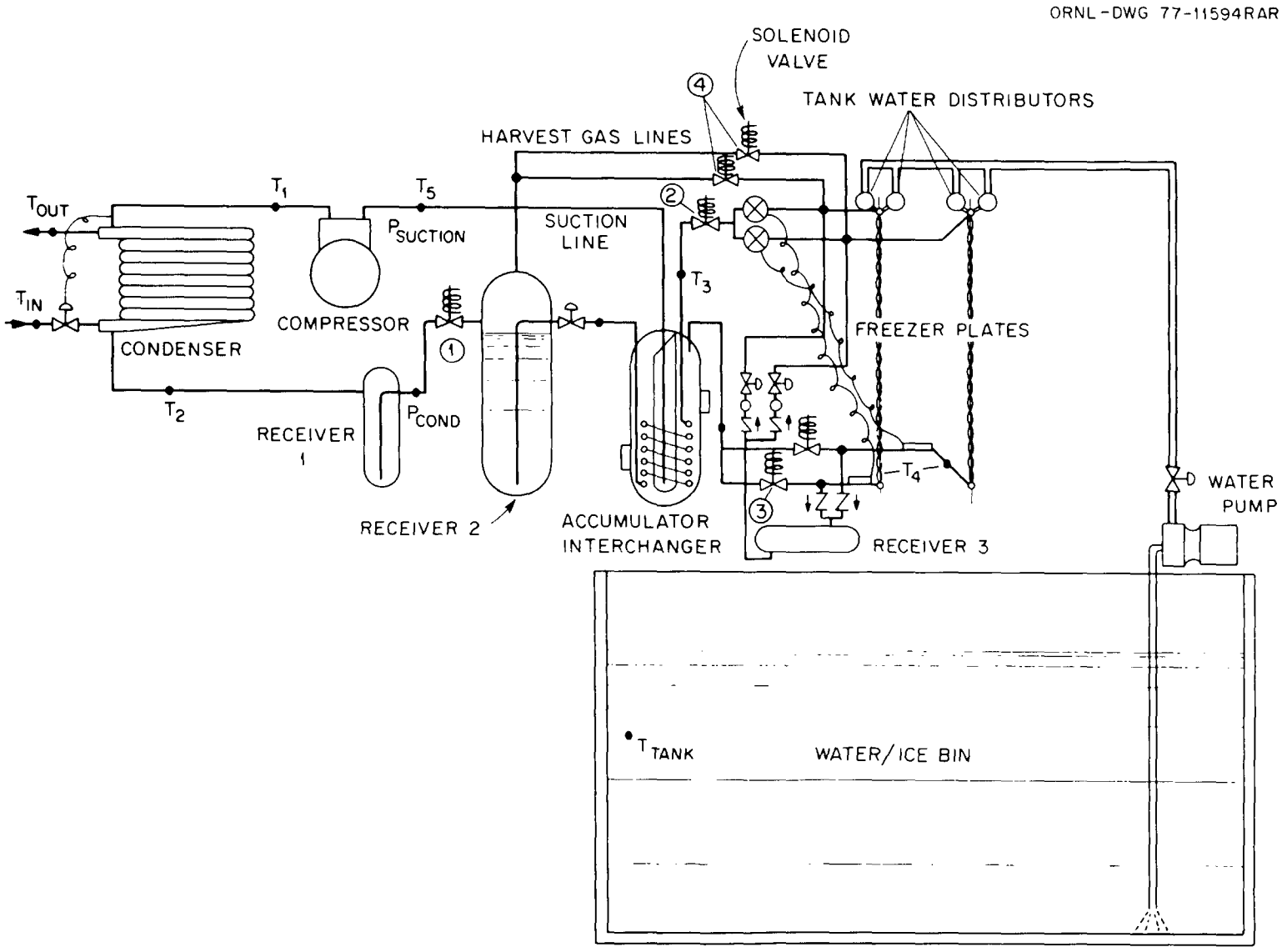

Fig. 8. Unit two schematic diagram.

ORNL-PHOTO 6216-77

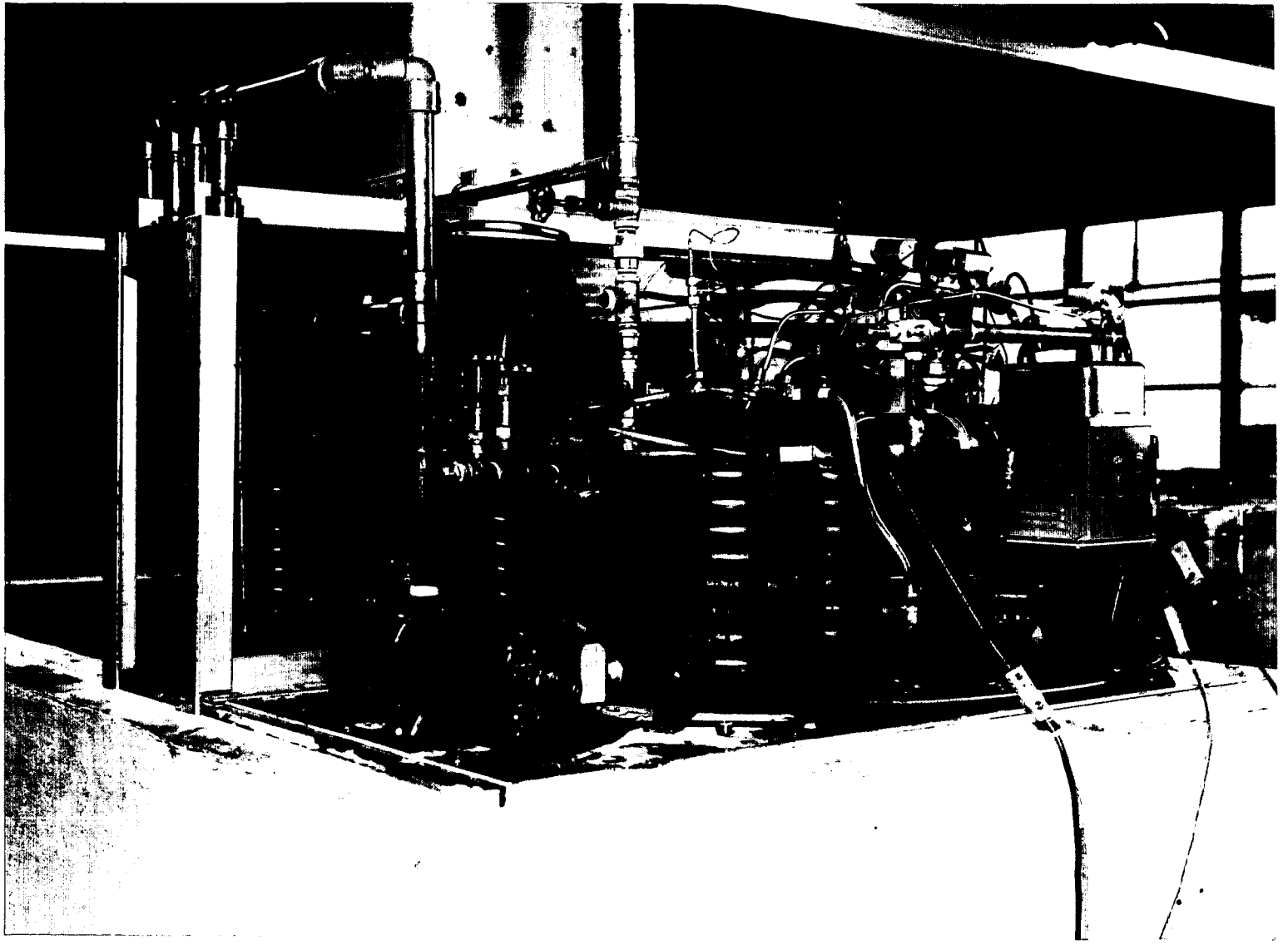

Fig. 9. Test unit two.

evaporator plate, where it condensed and caused the ice to slide into the storage tank. Condensed liquid was then routed through receiver 3 to the other plate, where some of it evaporated. The remaining liquid continued into the accumulator/interchanger, where it was boiled off by subcooling liquid during the following freeze cycle.

The typical freeze-harvest cycle of unit two has been described as follows:[6]

1. both plates freeze (typical time, 7.5 min);
2. first plate harvests while second plate continues to freeze (typical time, 35 s);
3. both plates freeze (typical time, 7.5 min);
4. second plate harvests while first plate continues to freeze (typical time, 35 s).

The length of the freeze-harvest cycle was varied by a timer, which allowed a maximum freeze time of 20.5 min.

Unit two was equipped with a slightly larger compressor from the same product line as that of unit one and an evaporator having 2.79 m^2 of active surface. The heating output of the unit was about 7325 W at a 41°C condensing temperature and −7°C evaporating temperature. This unit had an equalizing refrigerant circuit—that is, all pressures were equalized prior to start-up.

4.3 Test Unit Three

When testing was completed on unit two, it was dismantled to make room for unit three (illustrated schematically in Fig. 10). Figure 11 is a photograph of the system, which was equipped with a dual-fluid harvesting scheme.

Unit three's evaporator was composed of three copper plates, each having seven parallel flow circuits, 25.4 mm on centers (Figs. 12 and 13). Three of the circuits were used for the evaporating refrigerant, whereas the other four were used to circulate a warm 25% ethylene glycol/water brine solution for harvesting. During the freezing operation, refrigerant exiting the condenser passed through a coil submerged in the harvest-brine reservoir, thus subcooling the refrigerant and heating the brine solution between harvests. When harvesting, the compressor shut off and the refrigerant valve closed. The harvest pump circulated the warm brine from the top of the reservoir, through four circuits in each plate, and back into the bottom of the reservoir. Controls for the unit consisted primarily of two timers that allowed freeze times of up to 10 h and a maximum harvest time of 5 min. The unit was tested to maximum freeze times of 75 min; harvest generally took 2 to 3 min.

Unit three had a total evaporator area of about 5.57 m^2. Although the compressor and condenser from unit two were used with unit three, it had a slightly higher capacity, about 7900 W, for the same conditions. The refrigerant circuit was nonequalizing.

4.4 Test Unit Four

Unit four was essentially the same as unit one except for its harvesting scheme. Shown schematically in Fig. 14 and pictorially in Fig. 15, the unit used all the components of unit one except the hot-gas lines and the solenoid valves that controlled them. A dual-fluid-type harvesting scheme was added.

The harvesting scheme used a tank containing about 75 kg of water. During the freezing operation, the water was heated by subcooling the refrigerant. When harvesting was needed, valves 1 and 2 closed, the compressor shut off after a time delay of about 4 s, and valve 3 opened. The time delay allowed the compressor to pump any refrigerant in the accumulator to the receiver to prevent liquid floodback on restarting. With valve 3 open, the liquid refrigerant in the evaporator drained

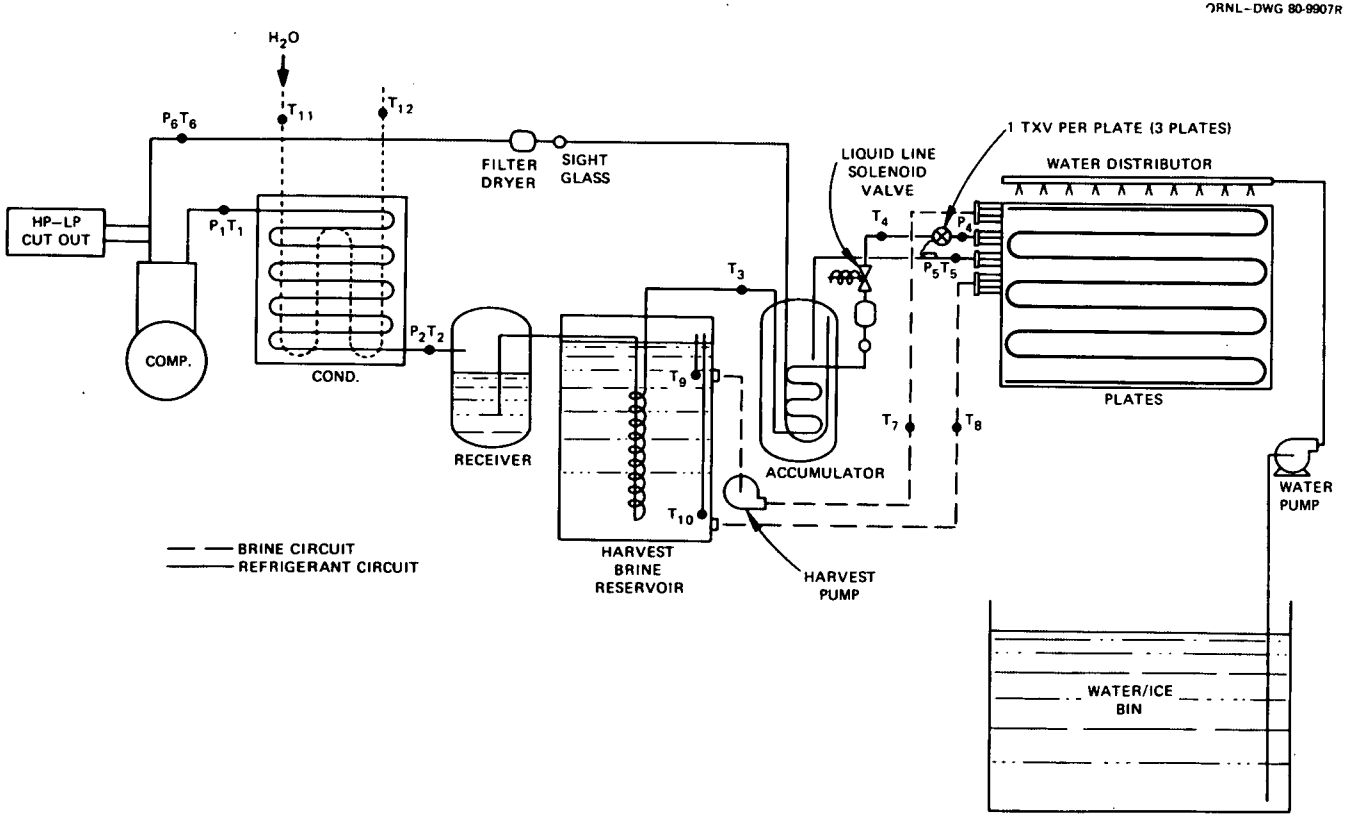

Fig. 10. Unit three schematic diagram.

ORNL-PHOTO 8055-79

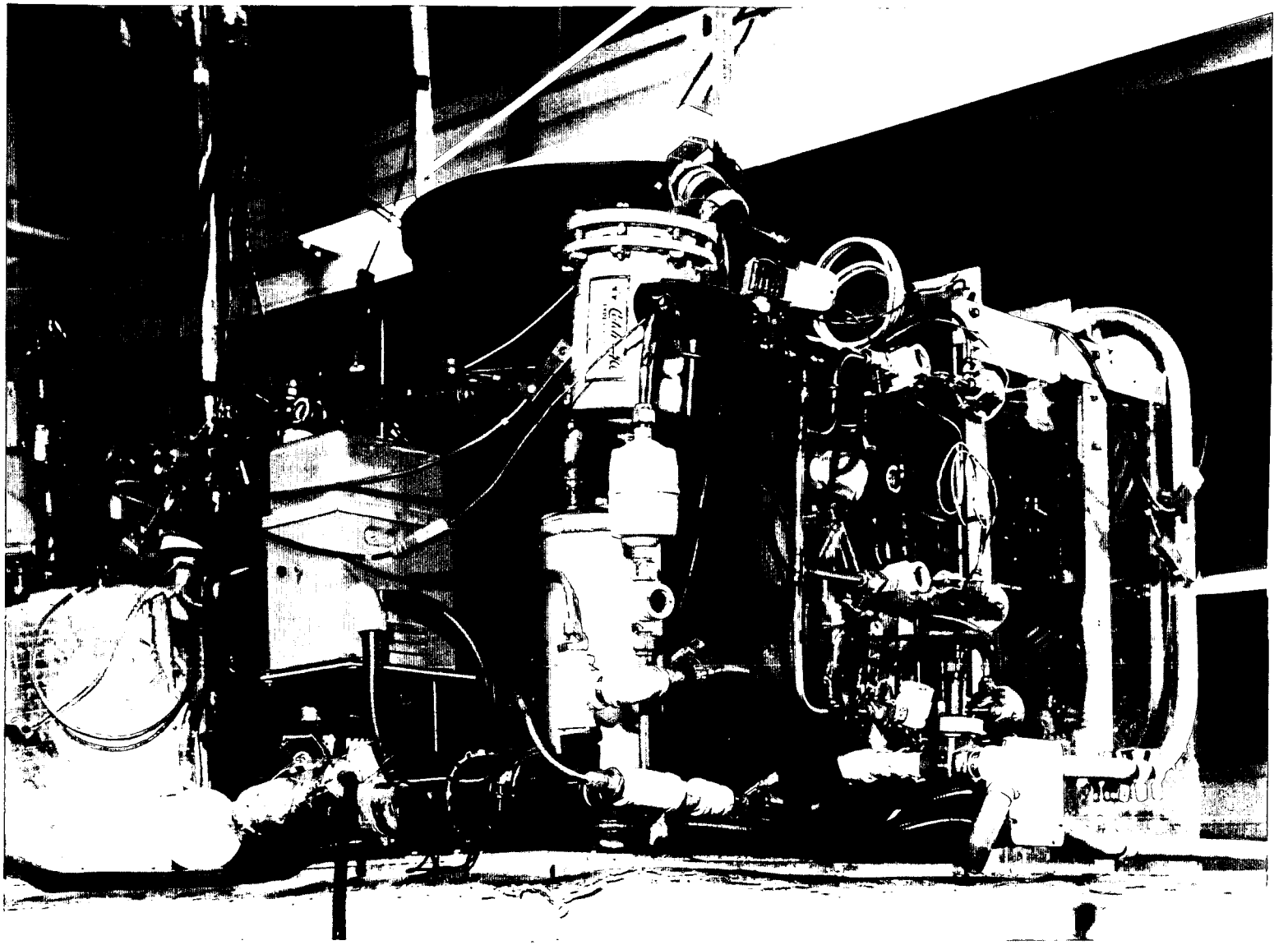

Fig. 11. Test unit three.

ORNL-DWG 80-9906

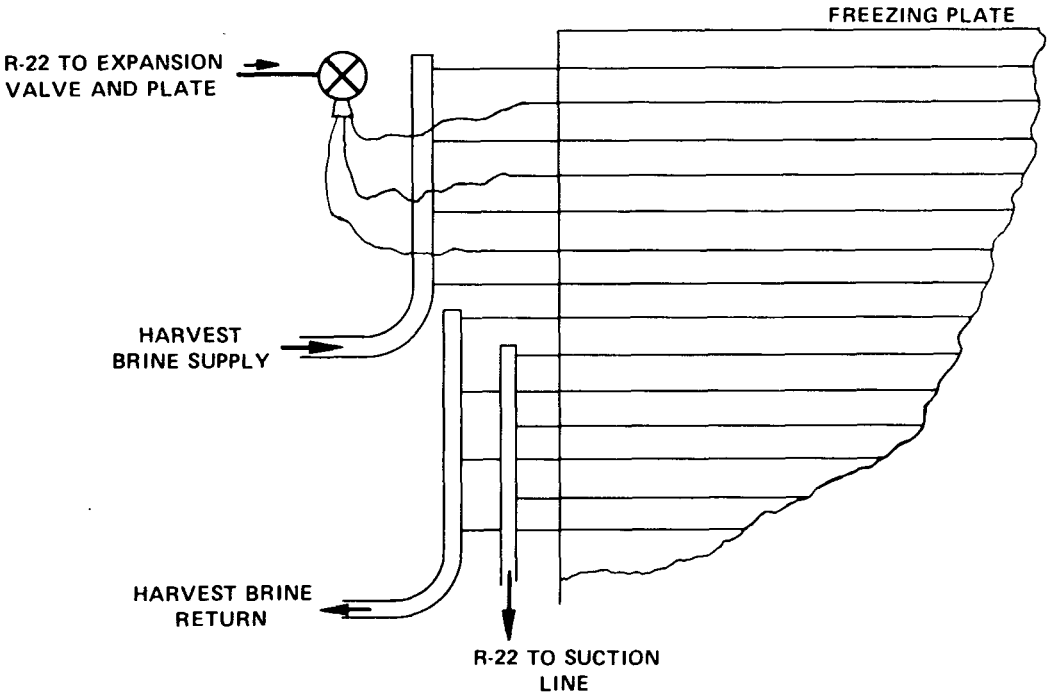

Fig. 12. Section of freezing plate from unit three showing details of harvest and refrigerant circuit manifolding.

ORNL-PHOTO 8056-79

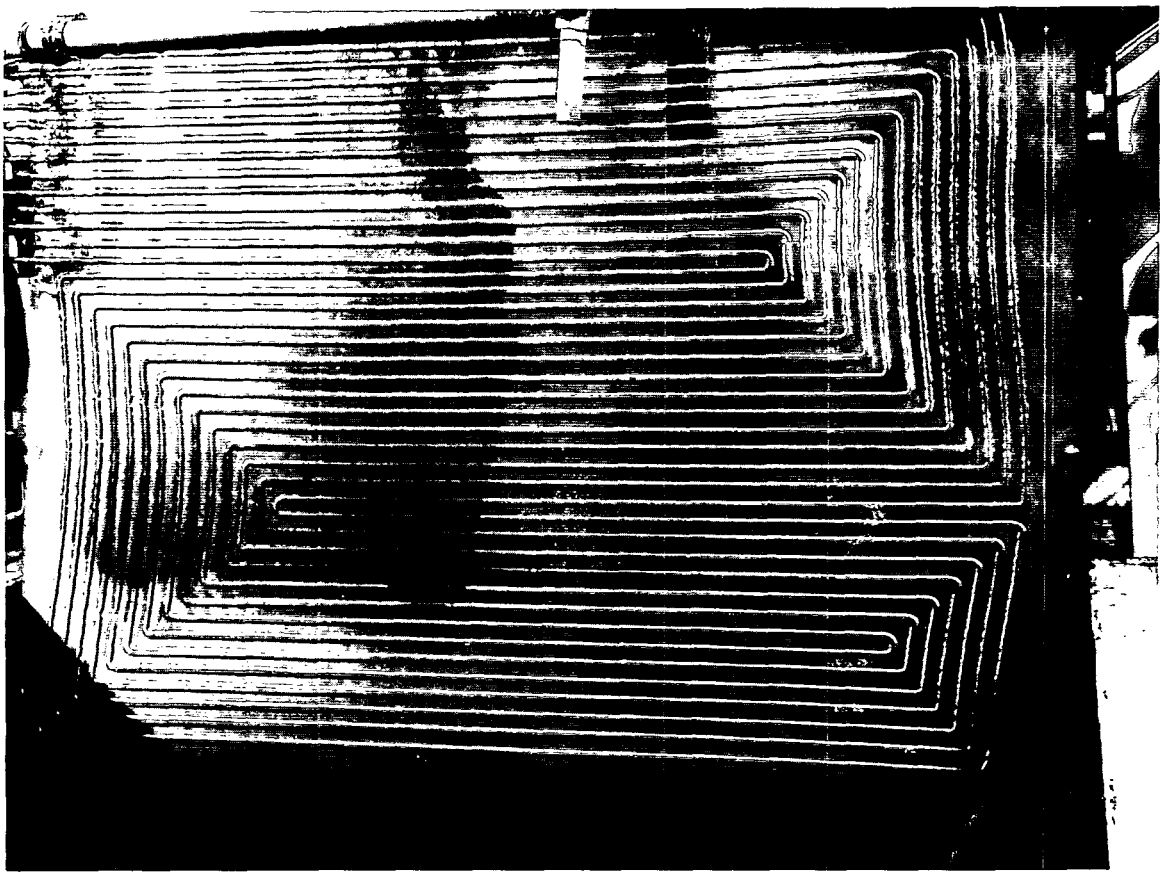

Fig. 13. Freezing plate from unit three.

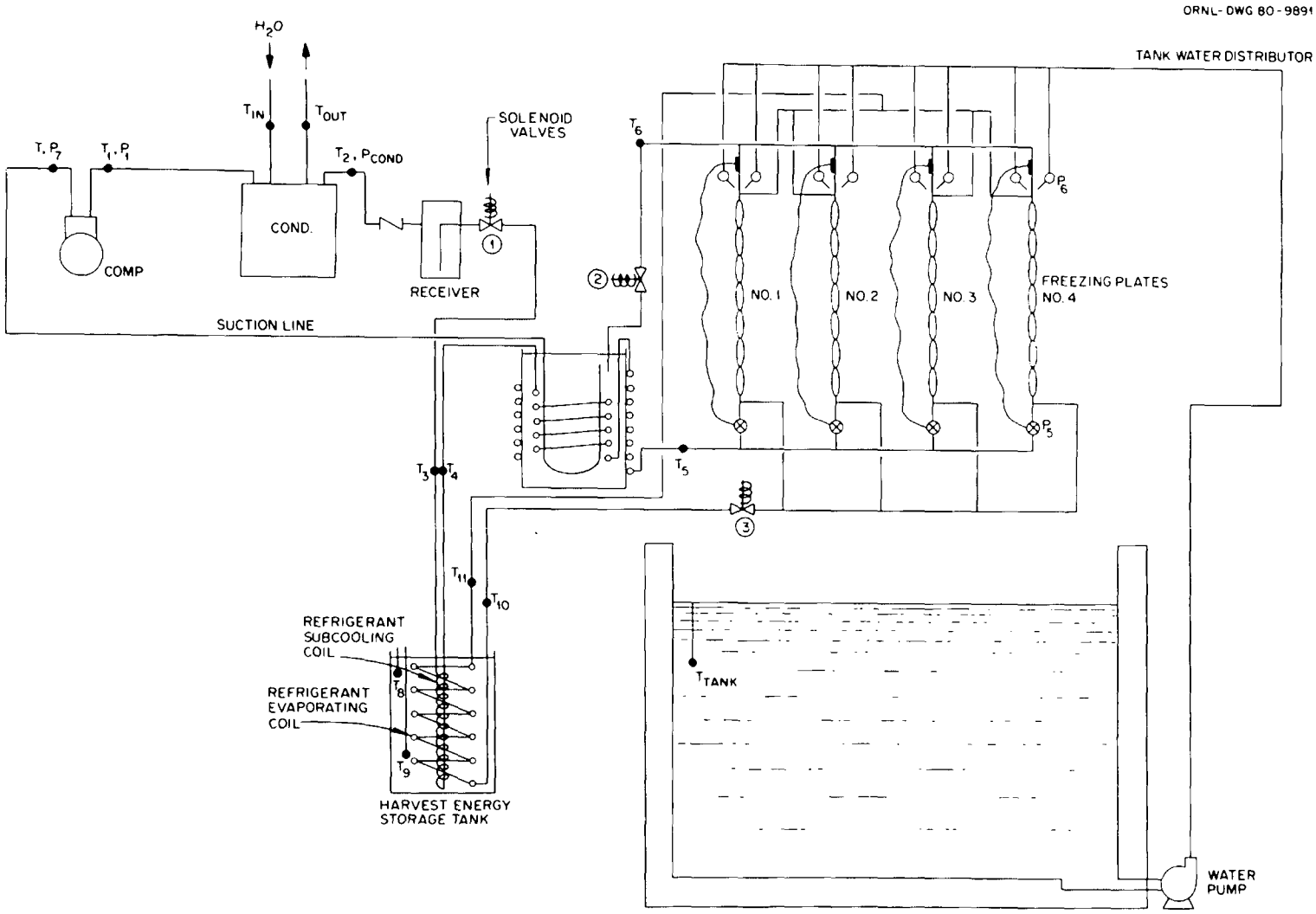

Fig. 14. Unit four schematic diagram.

ORNL-PHOTO 8053-79

Fig. 15. Test unit four.

down into the evaporating coil submerged in the harvesting reservoir. There, the refrigerant evaporated, and the vapor circulated back to the top of the plates and condensed, which completed the heat pipe circuit. Freeze-harvest cycles were controlled by a timer system that allowed freeze times of up to 10 h and harvest times of up to 10 min. During testing, the maximum freeze time was 2 h, and harvesting was usually done in 5 to 10 min.

The capacity of unit four and its evaporator size were the same as unit one. The refrigerant circuit was nonequalizing.

5. SYSTEM TESTS

The tests discussed in this section were conducted to evaluate the performance of the various harvesting schemes and their effect on overall system performance. The goal of the tests was to identify the most attractive scheme for use with IMHPs. Tests were conducted in both water-chilling and ice-making modes, and the effect of evaporator plate loading as well as harvesting scheme on system performance is discussed. Part-load tests were run to determine the performance degradation caused by cyclic operation.

Most of the tests were run with the evaporator plates exposed to room-ambient air at about 23.9°C; however, some testing was done at lower air temperatures to simulate more realistic operating conditions. The condensing temperature, unless otherwise specified, was 41°C.

The heating capacity of the heat pump was determined by measuring the condenser coolant temperature rise with copper-constantan thermocouples and by monitoring the total coolant flow with a water meter. Cooling capacity was estimated by performing heat balances on the refrigerant circuit. Compressor power consumption was measured with a Lincoln thermal watt converter and/or a watt-hour meter.

Refrigerant-cycle temperatures and pressures were measured by copper-constantan thermocouples attached to the tube surfaces and pressure gauges located as indicated in Figs. 5, 7, 9, 10, and 14. These data were taken to check cycle operation and for use in refrigerant-side heat balances.

All temperatures and the compressor power draw were recorded and averaged by the data acquisition system (DAS) described by Domingorena.[8] The DAS consisted primarily of a Digital Equipment Corporation PDP8/e mincomputer, an integrating digital voltmeter, a scanner, and an analog-to-digital converter.

5.1 Harvesting Scheme Evaluations

Table 1 gives harvest times for test units one (modified hot-gas scheme only), three, and four under various operating conditions. For freeze times of up to 20 min, and with the plates exposed to warm air, unit two harvest times ranged from 35 s (water pump running) to 1 min (pump off). The unit was not tested with the plates exposed to cold air.

Table 1. Harvest times for units one, three, and four

Freeze time (min)	Unit number	Harvest time (min)			
		23.9°C air		1.7–7.2°C air	
		Pump on	Pump off	Pump on	Pump off
10	1[a]	1.35		1.40	
	3	1.50		2.50	
	3	2.50		3.00	
30	1[a]	1.56		2.35	
	3	1.50		3.00	>5.00
	4	2.50		3.50	
60	1[a]	2.70		3.90	
	3	2.00		3.00	>5.00
	4	3.00	7.50	6.00	>10.00
90	4	4.00	8.50	8.00	>10.00

[a]Modified scheme.

5.1.1 Hot-Gas Harvest

Both hot-gas schemes tested on unit one harvested the plates quickly and thoroughly in laboratory tests; the average time was 45 to 50 s per plate. The performance of the modified hot-gas scheme (illustrated in Table 1 and Fig. 16) deteriorated markedly when the plates were enclosed in an insulated box. With a 16.7°C drop in air temperature, the harvest time nearly doubled. The effect of an uninsulated hot-gas line also caused harvest times to increase significantly. In all cases, the COP and capacity peaked at a freeze time of 20 min.

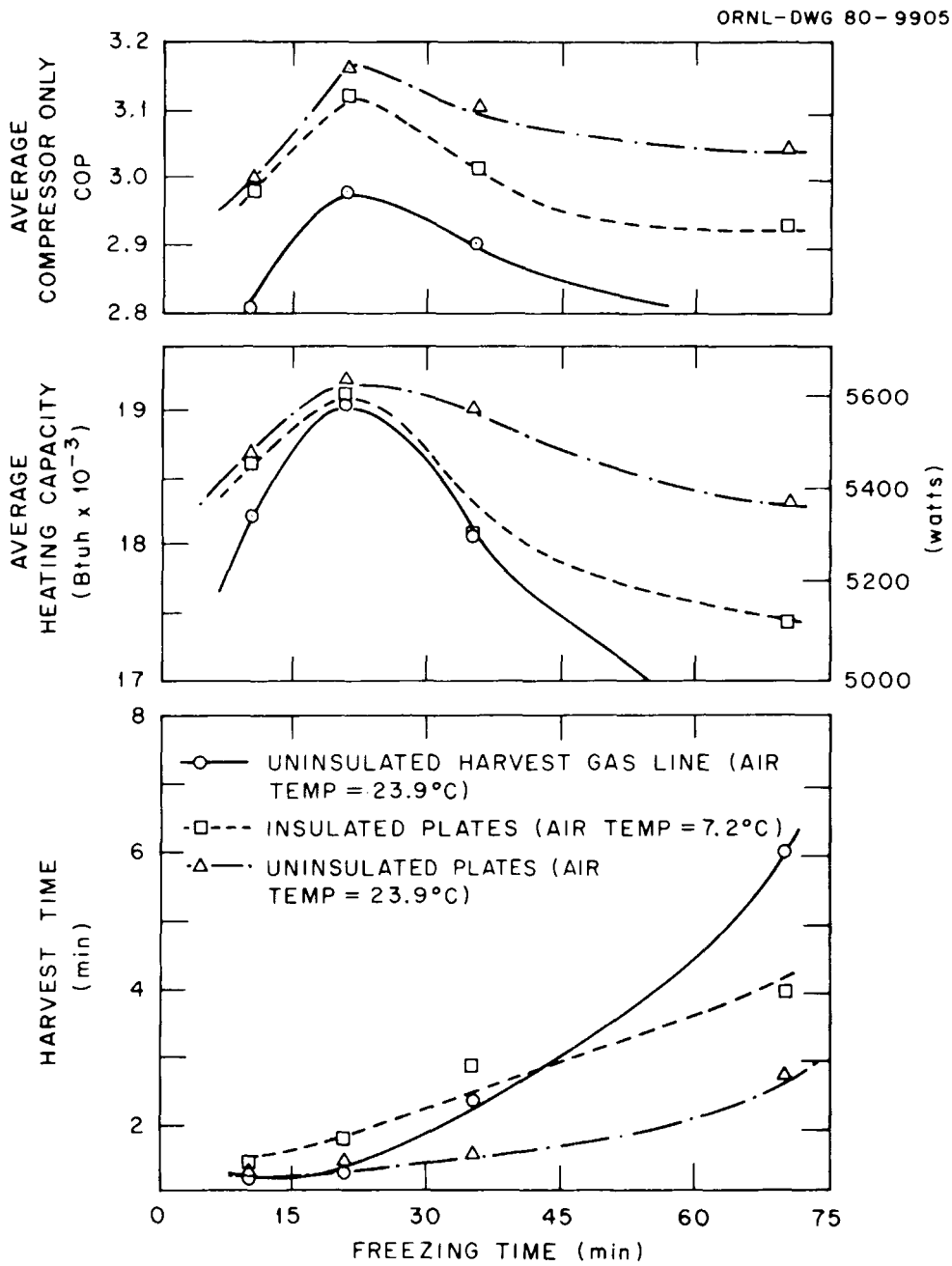

Fig. 16. Average COP, heating capacity, and harvesting time of unit one vs freeze cycle time for two ambient air temperatures.

Increased harvest time significantly degraded overall system performance, as illustrated in Fig. 16 and Table A.1.

Hot-gas harvesting is widely used in various applications, including air-to-air heat pumps, refrigerator-freezers, and frozen-food display cabinets. Although it does have the advantage of proven and available technology, the detrimental effect of hot-gas harvesting on thermal performance makes this scheme unattractive for use with IMHPs.

5.1.2 Stored-Refrigerant Harvest

The stored-refrigerant scheme of unit two harvested the plates in about 35 s or less, which makes it the fastest scheme tested. In addition, this scheme had little effect on the heating output of the unit because it was the only scheme that required no interruption of compressor operation.

Unit two required a minimum of 7.3 kg extra refrigerant charge to store the energy for defrosting. About 25% of this extra charge was condensed in the plates during each harvest. While the unit was in operation, most of this liquid was captured by the system accumulator. During off periods, however, the refrigerant tended to migrate to the coldest spot in the system. When this was the compressor and/or accumulator, the result was massive refrigerant floodback on start-up. In addition, problems with leaking solenoid valves often allowed the stored refrigerant in receiver 2 to migrate to the low side of the system, which compounded the floodback problem and caused harvesting failures. Eventually this refrigerant inventory control problem led to compressor failure because of lack of lubrication. This failure and continuous problems with harvesting-scheme control valves terminated the test program for unit two. Although the stored-refrigerant harvesting scheme offers some promise of being the fastest and most efficient, it is not considered attractive for IMHPs because of hardships imposed on system compressors by excess refrigerant inventory.

Another harvesting scheme that involves direct use of refrigerant for harvesting is the direct-subcooling harvest used on a dual-series evaporator heat pump.[7] (We did not test this scheme.) It appears to be reliable and does not need an extra-large charge, thus making it less liable to compressor problems. However, during harvesting, the subcooling liquid fills the evaporator plate. Upon resumption of the freezing operation, all of this liquid rushes into the accumulator at once, making refrigerant floodback possible. More information on this scheme can be found in ref. 7.

5.1.3 Dual-Fluid Schemes

Table 1 lists the experimental harvest times for the dual-fluid, off-cycle schemes used by units three and four, along with those of unit one's modified hot-gas scheme. Harvest times for both units were comparable to those of the hot-gas scheme; unit four required somewhat longer for harvesting than did the others. The sharp increase in harvest times of unit four for freeze cycles longer than about 60 min was caused by ice forming around the edges of the plates.

Occasionally, unit three had a similar problem caused by its water distribution headers. (Figure 17 illustrates a plate with its two headers.) On one of the plates, the headers were located so close to the freezing surface that they became ice-locked during long freeze times. It was impossible to defrost the plate under these conditions. If left unattended, massive ice buildups would occur.

Harvesting for units three and four took more than twice as long when water circulation from bin to plates was interrupted. Similar observations have been made by Fischer.[6]

To harvest the plates, it was necessary to turn off the compressors of both units during the harvesting period. However, it is felt that in most practical applications the control logic could be set

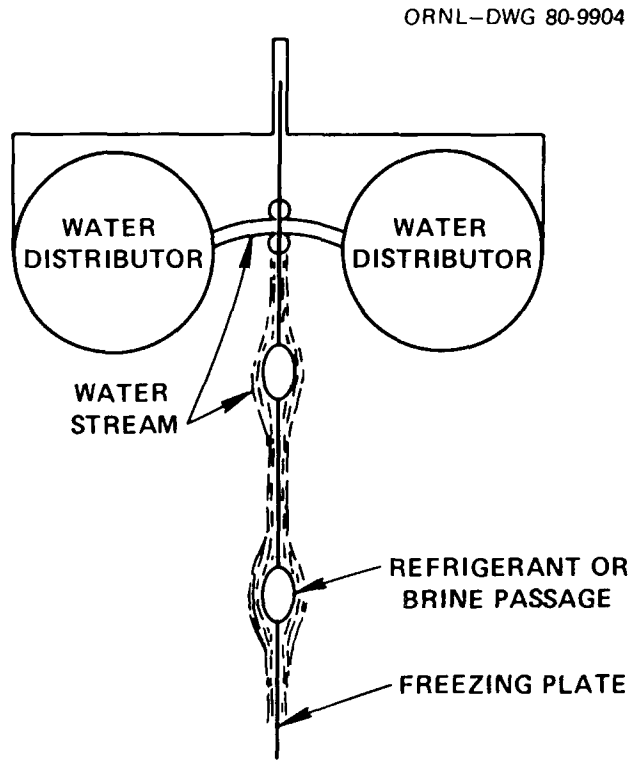

Fig. 17. Section of freezing plate on unit three showing relative location of water distributors.

to initiate the harvesting cycle, when necessary, upon normal compressor shutoff or after some maximum compressor on time. This should minimize the impact on the heating output of such a system.

Dual-fluid schemes have a number of advantages over the other harvesting schemes, including much simpler refrigerant circuits with fewer valves and fittings in the system. In addition, the refrigerant charge requirement is smaller, resulting in the practical elimination of refrigerant floodback problems caused by the harvesting scheme.

Reliable operation, negligible impact on system performance, and absence of refrigerant floodback and control problems make dual-fluid schemes the most attractive ones for IMHP applications. Of the two dual-fluid schemes tested, the dual-circuited-plate, pumped-brine system is recommended because of its shorter harvest times.

5.2 Plate-Loading Evaluations

Testing for plate-loading effect was done in two ways: (1) unit two was tested with a variable-speed open compressor, and (2) unit one was tested with variable evaporator area.[5] Figure 18 illustrates results of test data taken on unit two in the water-chilling mode.

The refrigerant COP in the upper curve is determined by performing a heat balance on the refrigerant circuit. It is calculated by the following:

$$\mathrm{COP}' = \frac{\text{heating output}}{\text{energy input to refrigerant stream by compressor}} .$$

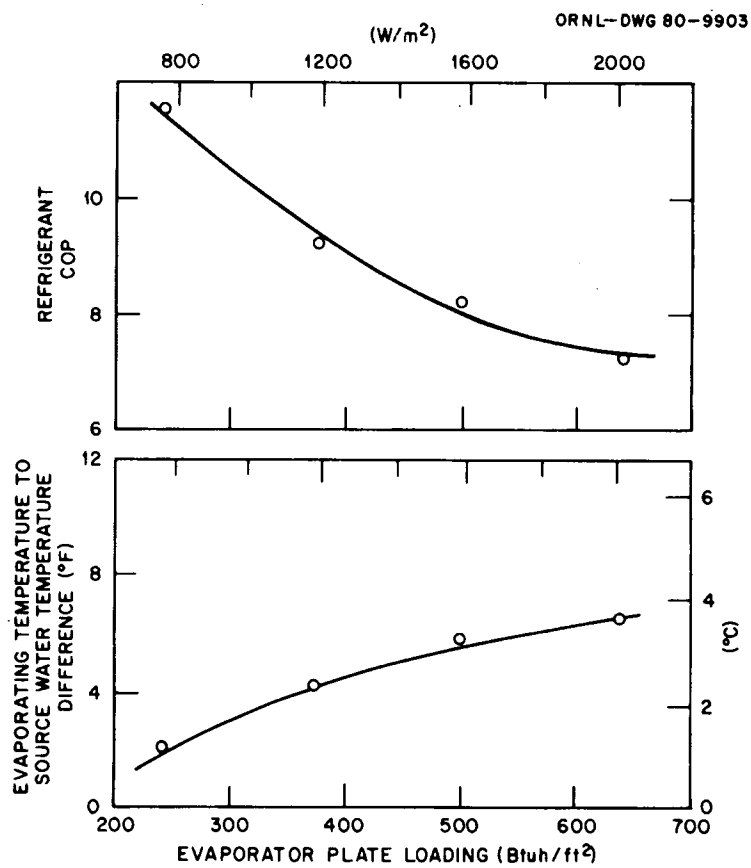

Fig. 18. Plate-loading test results on unit two with variable-speed open compressor.

Tank temperature was maintained at 6.7°C for these tests. Figure 19 shows that reducing the plate loading on unit one from 2800 to 1400 W/m^2 results in a 50% increase in its ice-making-mode COP. More complete tabular data can be found in Tables A.2 and A.3.

Results of both tests show that, for lower plate loading, evaporator temperature difference is lower and COP is higher. Therefore, plate loading for IMHPs, when in the ice-making mode, should be no greater than 1400 W/m^2, if economically possible.

5.3 System Performance Tests

5.3.1 Water-Chilling Tests

Test results presented in this section compare the water-chilling performance of units three and four with that of units two and one, respectively. The effects of plate loading and harvesting scheme on performance are discussed.

Procedure. The units were first allowed to reach steady-state operating conditions; then, a series of 1-h tests was run. Tank-water temperature, refrigerant system temperature, and power consumption were recorded each minute by the laboratory DAS. Refrigerant system pressures were read from gauges, and condenser cooling water flow was read from water meters.

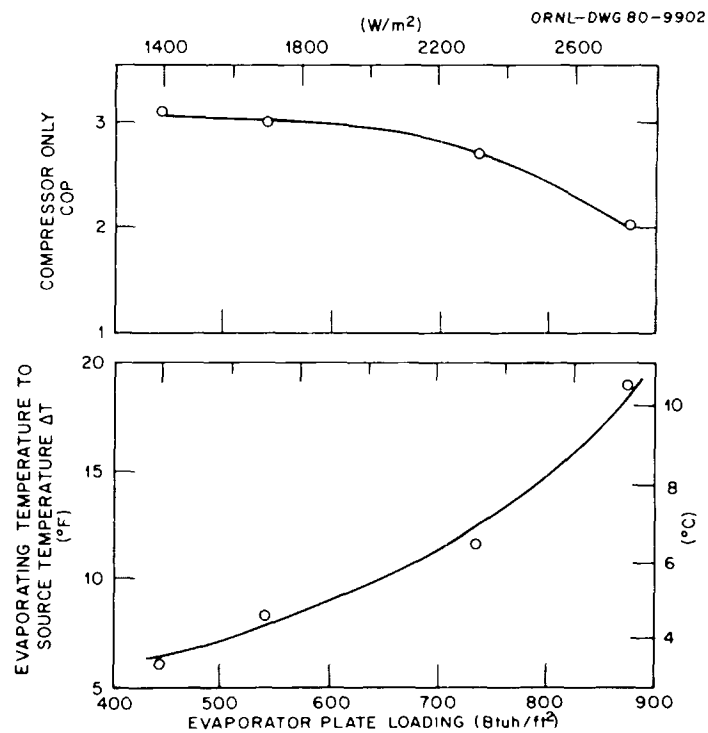

Fig. 19. Unit one average COP and evaporator temperature difference vs evaporator plate loading.

Results. Results of water-chilling performance tests are illustrated in Fig. 20 for units one and four and in Fig. 21 for units two and three. Tabular data from these performance tests are given in Tables A.4 and A.5.

The bottom half of Fig. 20 shows that, for a given tank-water temperature, the average evaporating temperature of unit four was slightly higher than that of unit one despite the fact that both used the same evaporator heat exchanger. However, unit one had a slightly higher COP (see upper half of Fig. 20). A possible reason for this occurrence is that the subcooling coil for harvest-energy storage added about 13.7 m of extra liquid line to the circuit. This induced some additional pressure drop, especially at the higher capacities associated with warmer tank-water temperatures, and resulted in somewhat lower performance values.

Figure 21 shows that unit two performed better in the water-chilling mode than did unit three, even though unit two had about twice the plate loading of unit three. This better performance was attained because the evaporator plates of unit three had very small (9.5-mm OD) flow passages, and, because of harvesting requirements, only three passages per plate were used for evaporation. This situation induced pressure drops in the evaporator alone in excess of 69 kP. The net effect was to produce a lower suction pressure for a given water temperature than was observed for unit two, thus eliminating unit three's plate-loading advantage. A better evaporator design with larger flow passages, which could eliminate this problem, is recommended for IMHPs for which a significant amount of operation in the water-chilling mode is expected.

5.3.2 Ice-Making Tests

Ice-making-mode testing was performed to compare the performance of these test units as a function of freeze time. The effects of harvesting scheme and plate loading on system performance are discussed.

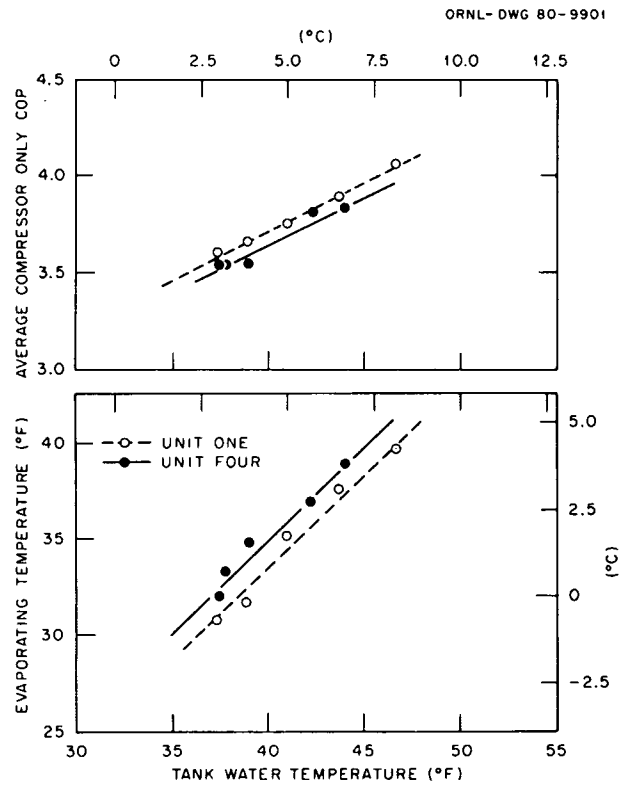

Fig. 20. Average evaporating temperature and COP vs tank-water temperature for units one and four.

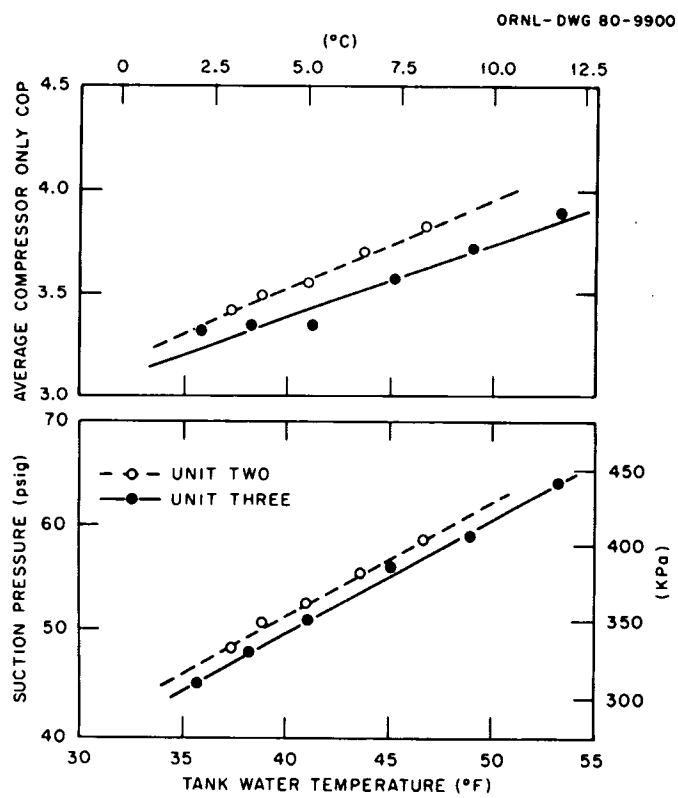

Fig. 21. Average suction pressure and COP vs tank-water temperature for units two and three.

Procedure. The procedure followed in the variable freeze-cycle-length tests was to run for 1 h or two cycles per test, whichever was longer. Temperatures and power-use rates were recorded each minute by the DAS. Refrigerant pressures were read from gauges, and condenser coolant flow was measured with water meters. For the steady-freeze tests, the units were started with plates clear of ice and allowed to build ice for 2 h. Data were taken as before.

Results. Figure 22 illustrates the performance of the units as a function of freeze-cycle length. Steady-freeze, no-harvest test results are shown in Fig. 23. Numerical results are tabulated in Tables A.6 and A.7.

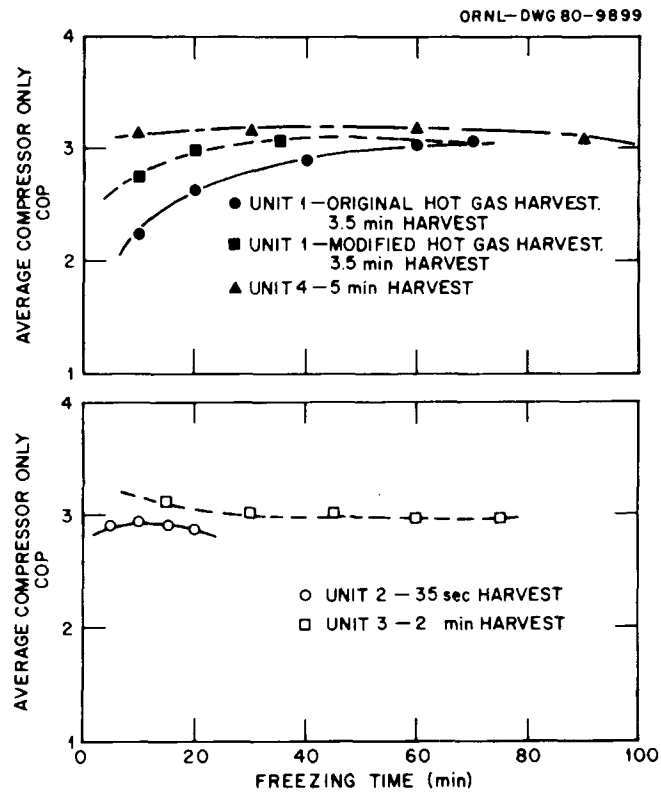

Fig. 22. Average COP vs freeze-cycle length for various IMHP test units.

The upper curve in Fig. 22 clearly shows that the hot-gas harvesting schemes used by unit one imposed significant penalties on the performance of that unit, particularly for short freeze cycles. Unit four experienced no such performance penalty. In fact, the off-cycle harvesting unit exhibited higher performance levels for all freeze-cycle lengths tested. Units two and three are compared in the lower curve, which indicates a distinct performance advantage for unit three. Harvesting did not significantly penalize heating output in either unit. However, unit three had about twice as much evaporator area and therefore only one-half the plate-loading level of unit two. At the lower evaporator temperatures and capacities associated with ice making, the evaporator pressure-drop penalty was not as great as it was in the water-chilling mode; thus, the plate-loading advantage was not completely negated. Therefore, unit three was able to maintain higher performance levels over a wider range of freeze-cycle lengths than was unit two, even though the same compressor-condenser combination was used in both units.

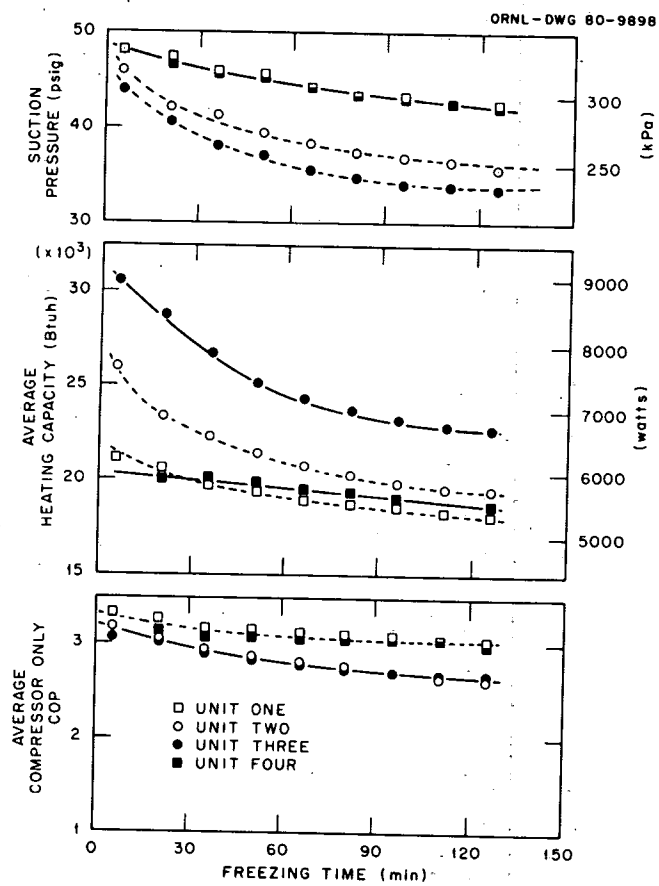

Fig. 23. Average COP, heating capacity, and suction pressure vs freeze time.

Figure 23 illustrates the effects of extended freeze-cycle time on COP, suction pressure, and heating output. Heating output for units one and four was essentially the same, and unit three exhibited a significantly higher output than unit two. This effect was probably because unit three had twice as much evaporator heat exchanger area as unit two. The apparently lower performance of unit three in steady freeze as opposed to freeze-harvest cycle operation was because the thermal expansion valves were set to a lower superheat value for the former test. This resulted in a more flooded evaporator, more rapid ice buildup, and, therefore, a lower evaporating temperature and COP.

Tests run on unit three with plates and bin insulated from the surroundings show the effect of air temperature around the plates on IMHP performance. As illustrated in Fig. 24, for an air temperature of 1.7°C, average capacity and COP are about 2% lower than the values for an air temperature of 23.9°C. Plate loading increased by about 2%. Wendschlag's[9] test results indicate that this performance and capacity reduction are caused by increased plate loading, which induces more rapid ice growth and, therefore, lower evaporating temperatures.

5.3.3 Cyclic Tests

Procedure. Cyclic tests were run on units three and four at rates of 0.3 to 6 cycles per hour (cph) and compressor-percent on times of 10, 20, 50, and 80%. Ice harvesting was accomplished during the off cycles of each test. Test duration was 1 h or two complete cycles, whichever was longer.

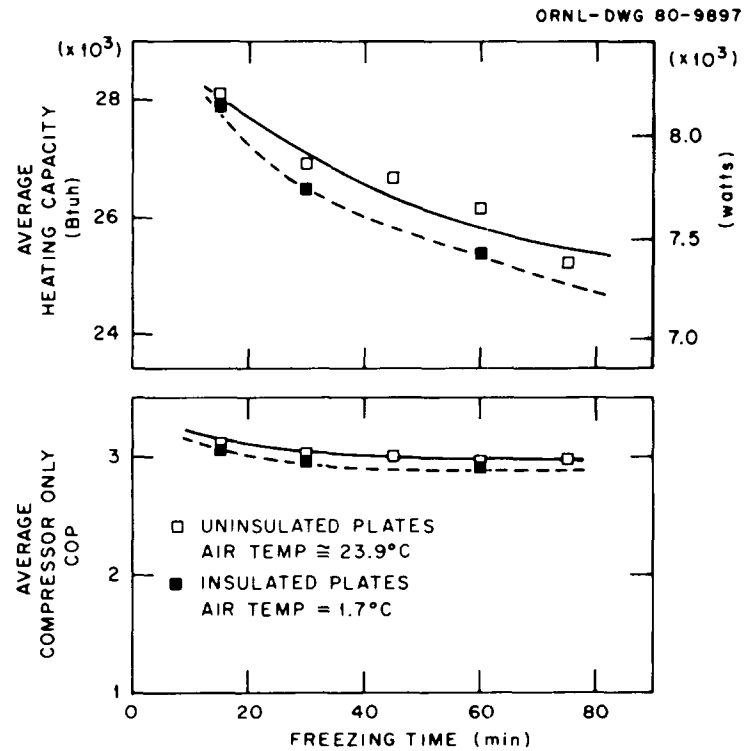

Fig. 24. Average COP and heating capacity of unit three as a function of air temperature and freeze-cycle length.

Results. Table 2 and Fig. 25 illustrate the results of the cyclic tests. The part-load factor PLF listed in the tables is defined as

$$\mathrm{PLF} = \frac{Q_{oc}}{Q_{oss} \times \Delta t},$$

where

Q_{oc} = total heat output during test, Wh,
Q_{oss} = steady-state full load heat output rate for a freeze time of 1 h, W,
Δt = total test duration, h.

The steady-state COP (COP_{ss}) was that measured during a 1-h freeze cycle, and the cyclic COP (COP_c) was the compressor-only heating COP measured during each test. A sample calculation is included in Appendix B.

Results indicate a maximum performance degradation, as indicated by COP, of about 15% for unit three and about 40% for unit four at part loads of about 10%. As the PLF increased, the cyclic performance of both units slightly surpassed that of the full-load performance. This was caused by the lower insulating effect of the thinner ice sheets produced during the cyclic tests—a result of their shorter on times. In other words, for the shorter on periods of the cyclic tests, the units were operating with higher average evaporating temperatures. A similar effect was observed by Hise[10] during short-cycle tests of the ACES demonstration house heat pump. Cyclic performance curves for unit two, taken from ref. 5, are included in Fig. 25 for comparison. Unit two was an equalizing system; that is, all pressures in the refrigerant circuit were allowed to equalize during off cycles.

Table 2. Cyclic performance of test units three and four[a]

Percentage on time	On time (min) Per cycle	On time (min) Total	Cycles per hour	Heating output (Wh)	Load factor, PLF	COP_c	COP_c/COP_{ss}
			Unit three				
100	60	60	1	7,423	1.00	2.93	1.00
10	3	6	2	701	0.09	2.50	0.85
20	6	12	2	1,531	0.21	2.76	0.94
50	5	30	6	3,954	0.53	2.89	0.99
50	15	30	2	3,948	0.53	2.92	1.00
80	8	48	6	6,292	0.85	2.93	1.00
80	12	48	4	6,443	0.87	2.99	1.02
80	24	48	2	6,506	0.88	2.95	1.01
80	40	80	1.2	10,280	0.86	2.94	1.00
			Unit four				
100	60	60	1	5,923	1.00	3.16	1.00
10	3	6	2	399	0.07	1.98	0.63
10	20	40	0.3	3,439	0.09	2.61	0.83
20	3	12	4	899	0.15	2.28	0.72
20	6	12	2	872	0.15	2.19	0.69
50	5	30	6	2,734	0.46	2.77	0.88
50	7.5	30	4	2,562	0.43	2.57	0.81
50	15	30	2	3,035	0.51	3.11	0.98
80	8	48	6	4,970	0.84	3.25	1.03
80	12	48	4	4,970	0.84	3.27	1.03
80	24	48	2	4,857	0.82	3.19	1.01
80	40	80	1.2	8,109	0.82	3.22	1.02

[a]Test data taken at air temperature of 1.7°C.

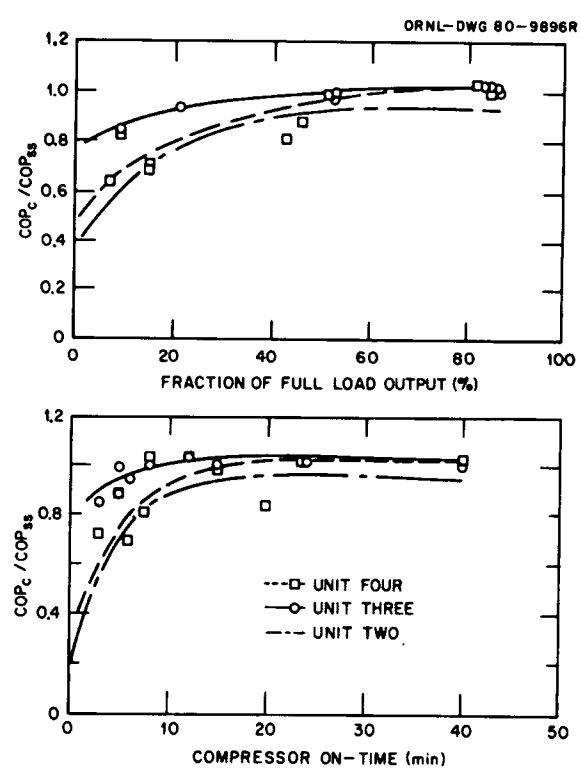

Fig. 25. Cyclic performance of units two, three, and four as a function of part load and on time.

Although its performance was close to that of unit four at low loads, unit two continued to experience noticeable performance degradations at part loads as high as 80%. This characteristic is attributed to pressure equalization and refrigerant migration to the evaporator side during the off cycle.

Several factors contributed to the rather significant performance degradation of unit four for very low loads and short on times. Although it was a nonequalizing system, its pumpdown cycle shutoff caused a vacuum to be pulled on the suction-line accumulator. On start-up, the system required about 1 min to adjust to the rapid pressure equalization in the suction line. During this time, a significant amount of two-phase flow was observed in the liquid-line sight glass, which indicated an insufficient supply of liquid for the evaporator. Another factor contributing to the performance degradation was loss of useful heat during the long off cycles associated with low load factors. During the on cycle, a temperature gradient was maintained between the condensing refrigerant and the cooling water, which made possible the removal of the useful heat product. During the off cycle, however, the hot water and refrigerant in the condenser tended to equalize thermally with the environment, thereby losing the useful heat produced during the on cycle.

Unit three was a nonequalizing system—that is, a pressure differential was maintained between the high- and low-pressure sides while the compressor was off. However, it underwent no pumpdown cycle and experienced no two-phase flow on start-up. The system's performance degradation was due primarily to the loss of useful heat caused by temperature equalization.

6. ICE-PACKING DENSITY

The ice-packing density—effective density of ice [in gm/cm^3 (lb/ft^3)]—produced by an IMHP and piled in a bin is an important parameter in the design of ice-storage bins for ACES or other systems employing low-side thermal storage. Obviously, the greater the packing density of the ice produced, the smaller the storage volume necessary and thus the lower the storage bin cost.

Ice-packing density is conveniently discussed in terms of the packing factor PF, defined as

$$PF = V_I / V_T ,$$

where V_I = ice volume in storage tank, and V_T = wetted volume of water and ice in storage bin.

The relationship of this packing factor to the weight-fraction packing factor PF_w can be shown by

$$PF = \frac{PF_w}{0.917 + PF_w \times 0.083} ,$$

where

$$PF_w = W_I / W_T = \frac{\text{weight of ice in bin}}{\text{total weight of ice and water in bin}} .$$

Details of the derivation are given in Appendix C.

The design packing factor of a coil-in-bin ACES with its cylinders of solid ice is 0.80. For IMHPs, with their free-floating sheets of ice, the packing factor is about 0.40.

This section deals with the results of ice-packing factor studies done on plate-type IMHPs and the brine-chiller system at the ACES demonstration house. The use of small amounts of ethylene glycol (0.25 to 1.35%) to weaken the ice and the results of a survey of the packing factors of several commercial ice makers are also discussed.

6.1 Test Procedure

For the ACES house brine-chiller system, the packing factor was determined by calculating the total weight of the water in the bin and the maximum ice inventory produced. Total water weight was calculated from bin dimensions and initial water depth. The rise in the bin water level was monitored to determine ice inventory.

Two types of tests, bucket sampling and bulk sampling, were used to determine packing factors for IMHPs.

Bucket-sampling tests involved filling a bucket with ice produced by the test units and weighing it. Then, the bucket was filled with 0°C water to the same level as the ice and weighed again. The packing factor was determined by

$$PF_w = PF_w' \times SF ,$$

and

$$PF = \frac{PF_w}{0.917 + PF_w \times 0.083} ,$$

where

PF = effective packing factor,
PF'_w = ice sample weight/total ice and water weight (apparent packing factor),
SF = fraction of sample that was solid ice as determined by calorimeter tests.

The solid-ice fraction SF is an indication of the energy density of the ice produced and must be used to modify the apparent packing factor to determine the concentration of solid 3.34×10^5 J/kg (144 Btu/lb) ice.

Bulk sampling involved running one of the test units for a week to fill one of the small laboratory tanks with ice. At the end of the week, the volume and maximum thickness of the ice pack were measured. After the ice pack melted, the level was measured to determine the total weight of ice produced. Packing factors were calculated as follows:

$$PF_B = \frac{W_I}{\rho_I V_B} \quad \text{(bin-volume-based packing factor)} ,$$

and

$$PF_I = \frac{W_I}{\rho_I V_I} \quad \text{(ice-volume-based packing factor)} ,$$

where

W_I = ice weight,
ρ_I = ice density at 0°C,
$V_B \equiv$ bin volume needed based on maximum ice thickness,
$V_I \equiv$ ice pack volume.

6.2 Test Results

6.2.1 Brine Chiller

Results of two winters of heating operation at the ACES demonstration house indicate that maximum packing factors achieved were 0.77 for 1977–1978[11] and 0.87 for 1978–1979.[12] Table 3 summarizes these results.

6.2.2 Plate-Type IMHP

Tables 4 and 5 respectively summarize the results of bucket- and bulk-sampling tests performed on the ice generated by the test units. The bucket-sampling method yielded an average effective packing factor of about 0.44. The ice-volume-based packing factors of the bulk samples averaged about 0.47. Modifying PF_I by the average solid-ice fraction of 0.848 yields an effective packing factor of 0.40 for the bulk-sampling tests, about 9% less than for the bucket samples. Averaging the results of these two methods yields an effective PF of about 42%.

Bucket samples simulate a bin scheme in which the ice is evenly distributed and floating in a water bath. Excessive piling or mounding of ice beneath the evaporator plates would be avoided by using this scheme.

Table 3. Maximum packing factors achieved in ACES house ice bin

	Total water inventory (t)	Maximum ice inventory (t)	PF_w	PF
1977–1978	68.62	51.65[a]	0.75	0.77
1978–1979	63.50	54.54	0.86	0.87

[a]Bin not quite filled to capacity.

Table 4. Bucket-sampling test results

Sample	Test unit	PF_w'	SF	PF_w	PF
1	1	0.45	0.803	0.36	0.38
2	1	0.47	0.814	0.38	0.40
3	1	0.49	0.876	0.43	0.45
4	1	0.47	0.933	0.44	0.46
5	3	0.51	0.873	0.45	0.47
6	1	0.55	0.795	0.45	0.45
7	1	0.51	0.845	0.43	0.45
8[a]	1	0.71	0.845	0.60	0.62
Average, excluding sample 8		0.49	0.848	0.42	0.44

[a]Compacted ice.

Table 5. Bulk-sampling test results

Sample	Test unit	Original water volume, V_w (m^3)	Ice-pack volume, V_I (m^3)	Bin volume needed, V_B (m^3)	Ice weight (kg)	PF_B	PF_I
1	2	1.00	2.03	2.78	850	0.33	0.46
2	2	1.13	2.40	3.28	1028	0.34	0.47
3	2	1.13	2.48	3.20	1012	0.34	0.45
4	1	1.74	4.02	4.91	1803	0.40	0.49
5	1	1.16	2.03	4.13	1016	0.27	0.55
6	2	0.51	0.93	1.52	425	0.31	0.50
7	2	0.65	1.52	2.34	5.67	0.26	0.41
Average						0.32	0.47

The bulk-sampling technique models the situation in which the storage bin is only partially filled with water, of which about 80% is then frozen. Although the bulk-method packing factor, as based on the ice volume, is not much less than that of the evenly distributed water-ice mixtures, the ice-pack mounding under the plates necessitates a larger amount of freeboard volume in a rectangular bin for containment. As indicated in Table 5, this degrades the packing factor by about 32%, from 0.47 to 0.32. In addition, the ice mounding can lead to harvesting failures if the mound comes in contact with the evaporator plates. Figures 26 and 27 show the large, irregularly shaped, corrugated sheets of ice produced by the plate-type IMHPs tested. The mounding phenomenon is particularly evident in Fig. 27. Figure 28 shows a typical cross section of one of the ice sheets. The side next to the plate surface is corrugated, and the water side is smooth.

ORNL-PHOTO 8058-79

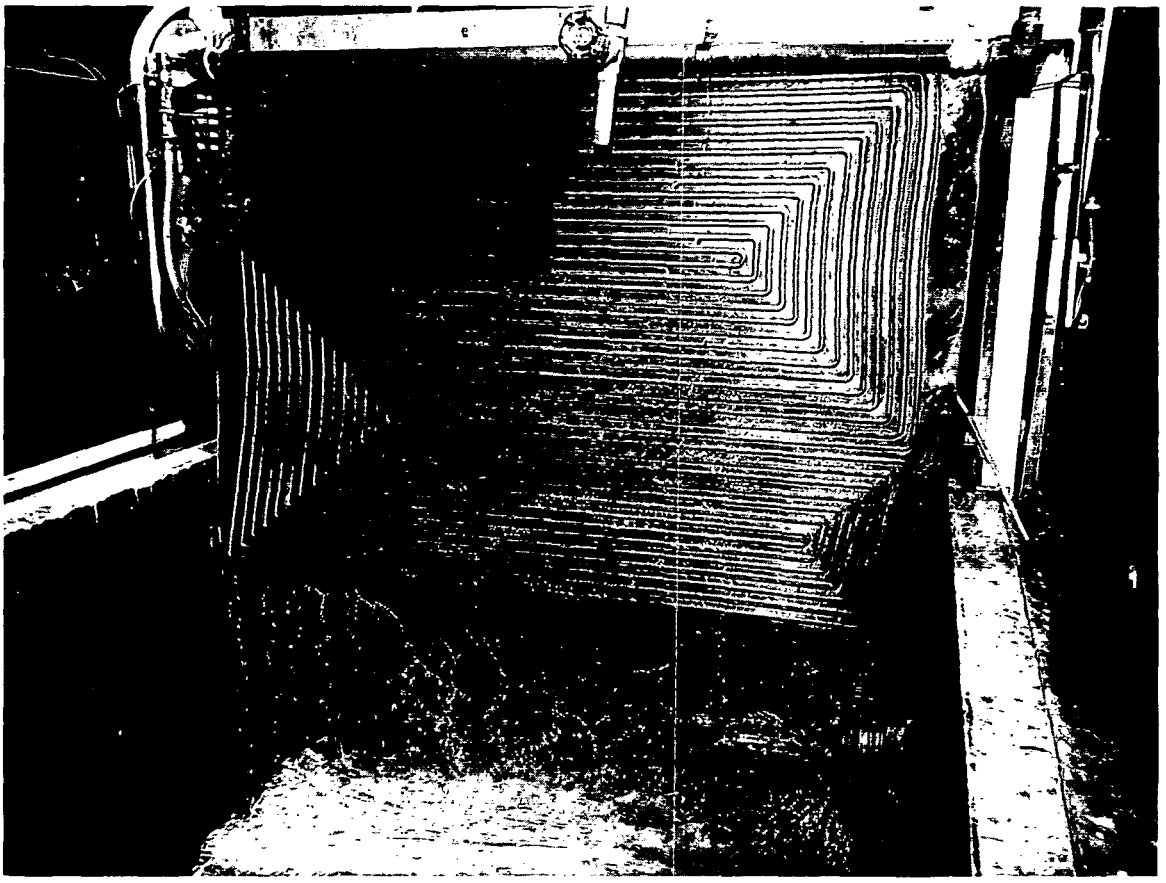

Fig. 26. Test unit three harvesting ice.

The scheme of even distribution of the ice in water, as modeled by the bucket-sampling technique, yields higher effective packing factors and avoids the formation of ice mounds, which require extra freeboard volume. Clearly, this scheme requires less bin volume for the same ice production and is therefore the recommended method for ice storage with IMHP systems. Sample calculations for the bucket- and bulk-sampling techniques are given in Appendix B.

6.3 Ethylene Glycol Treatment Results

The tank water was treated with ethylene glycol in an attempt to eliminate the harvesting requirement by weakening the ice so that it would not adhere to the evaporator surface and to improve the ice-packing density. The glycol concentrations used (0.25 to 1.35 vol %) did not weaken the ice sufficiently to prevent adherence to the evaporators. Higher concentrations that might loosen the ice would also lower the freezing temperature and reduce system performance; hence, this is not recommended.

Tables 6 and 7 give results of packing tests on ethylene glycol–treated bin water. Comparison with bucket-sampling results for untreated water indicate an increase in the apparent packing factor, accompanied by a decrease in the solid-ice fraction, or energy density, of the ice. The effective packing factor was not significantly altered. Bulk-sampling comparisons indicate a decrease in the bin-volume-based packing factor of about 10% for the treated case. Modifying the ice-volume-based packing factor by the solid-ice fraction yields an effective packing factor of 0.35 as compared with 0.40 for the untreated case.

ORNL-PHOTO 168210

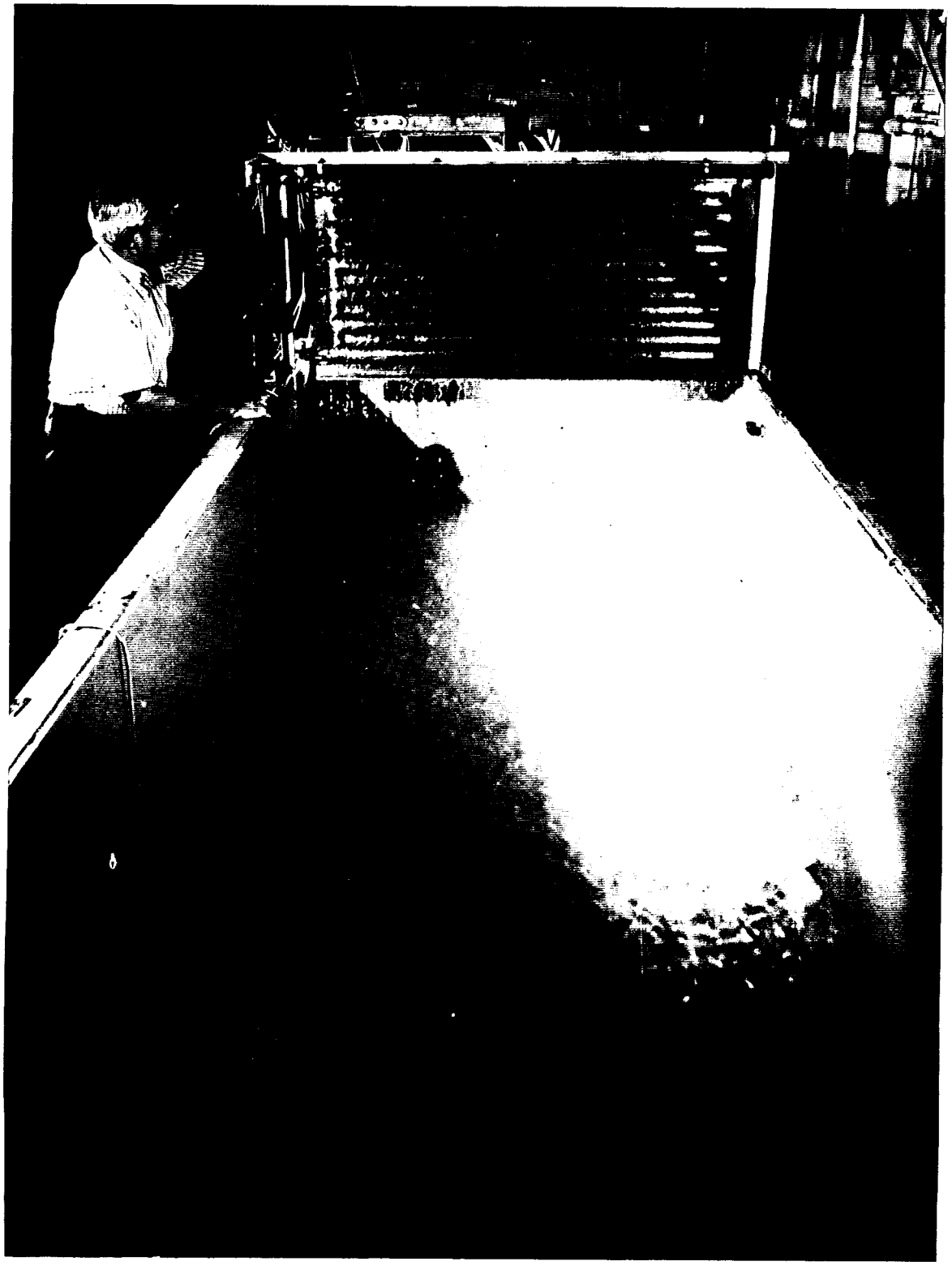

Fig. 27. Ice mound produced by IMHP during bulk-sampling test.

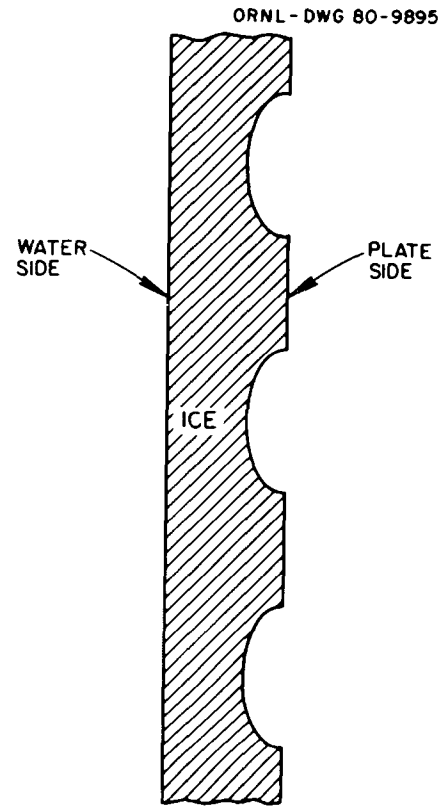

Fig. 28. Cross section showing typical IMHP ice geometry.

Table 6. Effect of ethylene glycol on bucket-sample packing factors

Percentage ethylene glycol	PF_w'	SF	PF_w	PF
0.5	0.56	0.65	0.36	0.38
0.63	0.66	0.71	0.47	0.49
0.84	0.59	0.68	0.40	0.42
1.10	0.64	0.60	0.38	0.40
1.35	0.67	0.63	0.42	0.44
Average	0.62	0.65	0.41	0.43

Table 7. Effect of ethylene glycol on bulk-sample packing factors

Percentage ethylene glycol	Original water volume, V_W (m^3)	Ice-pack volume, V_I (m^3)	Bin volume needed, V_B (m^3)	Ice weight (kg)	PF_B	PF_I
0.25	1.26	2.43	4.13	1262	0.34	0.57
0.50	1.26	3.02	5.38	1387	0.28	0.50
0.63	1.80	2.49	6.07	1415	0.25	0.62
1.35	1.70	1.97	3.85	846	0.24	0.47
Average					0.28	0.54

From the preceding discussions, it is evident that addition of ethylene glycol results in no improvement of the ice-packing factor, nor does it prevent adherence of ice to the evaporator plates. Thus, ethylene glycol treatment is not recommended.

6.4 Survey Results

Various commercial ice makers were surveyed to determine the effect of different ice geometries (cubes, cylinders, flakes, etc.) on packing factors determined by the bucket-sampling method. Test results given in Table 8 indicate that chipped or crushed ice yields no improvement in the packing factor. However, cylindrical and cubical shapes yielded packing factors of 0.58 to 0.66, an average improvement of more than 40% over the plate-type evaporator ice.

This increase in packing factor could possibly reduce storage costs for IMHP-based ACES, making them more competitive with the brine-chiller, coil-in-bin systems. However, evaporators designed to produce small cubes or cylinders of ice are more complex and more expensive than the flat-plate evaporators, which tends to counteract the beneficial effect of the increased packing factor. As an example, the evaporator of test unit three costs about $300. Conversations with distributors of ice-making equipment indicate that an evaporator of the same capacity, making cylindrical or cubical ice, would cost seven to ten times as much. Reference 13 provides a more complete discussion of the relative economics of various IMHP and brine-chiller ACES.

Table 8. Geometric effects on ice-packing factors

Ice shape	Sample	PF'_w	SF	PF_w	PF
Irregular, flat, thin (<3.0 mm) chips	1	0.50	0.81	0.41	0.43
	2	0.53	0.81	0.43	0.45
	3	0.58	0.81	0.47	0.49
Crushed flakes	1	0.50	0.75	0.38	0.40
	2	0.51	0.77	0.39	0.41
25-mm hollow cubes	1	0.35	1.00	0.35	0.37
12.5-mm solid cubes	1	0.64	1.00	0.64	0.66
12.5 × 16 × 16 mm solid rectangles	1	0.59	1.00	0.59	0.61
25 × 38 mm solid cylinders	1	0.59	1.00	0.59	0.61
25 × 25 mm solid cylinders	1	0.56	1.00	0.56	0.58
25 × 6 mm solid spherical section	1	0.59	1.00	0.59	0.61
Plate-type IMHP ice; large corrugated sheets[a]		0.49	0.85	0.42	0.44
Brine-chiller ice,[b] submerged solid cylinders		0.75–0.86		0.75–0.86	0.77–0.87

[a]Averages from Table 4.
[b]Included for comparison.

7. CONCLUSIONS

As a result of the IMHP development program, several conclusions have been reached about IMHP systems:

1. A dual-fluid harvesting scheme, which stores energy for harvest in a secondary fluid medium, is the best defrosting scheme tested for IMHPs.
2. Of the two dual-fluid harvesting schemes tested, the dual-circuited-evaporator, pumped-brine system has the shortest defrosting times and the simplest refrigeration circuit. It is recommended over the heat pipe system.
3. Evaporator plate loading should not exceed 1400 W/m^2 during the ice-making mode.
4. Refrigerant circuits should be nonequalizing to minimize cyclic losses.
5. Arranging the control logic to initiate harvesting during normal off periods will reduce the need to interrupt operation for defrosting.
6. Distributing the ice evenly in the water/ice storage bin by floating it in water yields minimum tank sizes for IMHP systems.
7. Solid cubes or cylinders of ice require smaller tank sizes, but such evaporators are more complex and more expensive and are, therefore, not recommended.
8. Plate-type IMHP-based systems would require twice as much bin volume as brine-chiller-based systems for the same energy storage capacity.

REFERENCES

1. H. C. Fischer et al., *The Annual Cycle Energy System; Initial Investigations,* ORNL/TM-5525 (October 1976).

2. H. C. Fischer and E. A. Nephew, "Application of the Ice-Maker Heat Pump to an Annual Cycle Energy System," paper presented at ASME Winter Annual Meeting, New York (December 1976).

3. E. C. Hise, J. C. Moyers, and H. C. Fischer, *Design Report for the ACES Demonstration House,* ORNL/CON-1 (October 1976).

4. A. S. Holman and V. R. Brantley, *ACES Demonstration: Construction, Startup, and Performance Report,* ORNL/CON-26 (October 1978).

5. V. D. Baxter, *Intermediate Report on the Performance of Plate-Type Ice-Maker Heat Pumps,* ORNL/CON-23 (October 1978).

6. H. C. Fischer, *Development and Testing of a Single-Plate and a Two-Plate Ice-Maker Heat Pump,* ORNL/CON-21 (April 1978).

7. Gary Mondry, *The Effect of Subcooling on the Performance of a Dual-Series Evaporator Heat Pump,* Senior Thesis, Bulletin No. 74-06-EES-04, University of North Dakota, Grand Forks, 1979.

8. A. A. Domingorena, *Performance Evaluation of a Low-First-Cost, Three-Ton, Air-to-Air Heat Pump in the Heating Mode,* ORNL/CON-18 (October 1978).

9. James Craig Wendschlag, *Isothermal Heat Transfer Through a Thin Fluid Film Undergoing a Phase Change with a Secondary Heat Transfer from a Warm Environment,* Masters Thesis, Bulletin No. 79-06-EES-02, University of North Dakota, Grand Forks, 1979.

10. E. C. Hise, *Performance Report for the ACES Demonstration House, August 1976 Through August 1977,* ORNL/CON-19 (March 1978).

11. A. S. Holman et al., *Annual Cycle Energy System (ACES) Performance Report, November 1977 Through September 1978,* ORNL/CON-42 (May 1980).

12. V. D. Baxter, *Annual Cycle Energy System (ACES) Final Performance Report, December 1978 Through September 1980* (in preparation).

13. R. E. Minturn et al., *ACES 1979: Capabilities and Potential,* ORNL/CON-48 (May 1980).

APPENDIX A

TABULATED TEST RESULTS

Tables A.1 through A.7 present results of laboratory testing of ice-maker heat pump units one, two, three, and four.

Table A.1. Performance of unit one with modified hot-gas harvesting scheme

Freeze time (min)	Air temperature (°)	Heating capacity (W)	Plate loading (W/m^2)	COP	Harvest time (min)	Refrigerant flow rate (kg/h)
10	23.9[a]	5342	1271	2.81	1.24	88.9
	7.2	5456	1258	2.98	1.40	89.8
	23.9	5466	1258	3.00	1.35	89.8
20	23.9[a]	5584	1274	2.98	1.28	88.0
	7.2	5590	1258	3.12	1.73	90.3
	23.9	5624	1240	3.16	1.42	90.3
35	23.9[a]	5298	1217	2.90	2.34	85.3
	7.2	5297	1199	3.01	2.85	85.7
	23.9	5570	1224	3.10	1.56	88.4
70	23.9[a]	4756	1145	2.74	6.04	79.4
	7.2	5104	1167	2.93	3.94	82.6
	23.9	5366	1221	3.04	2.70	85.6

[a]Hot-gas line uninsulated.

Table A.2. Plate-loading test results using variable-speed open compressor on unit two[a]

Compressor speed (rpm)	Plate loading (W/m^2)	Suction pressure (kPa)	Specific refrigerant flow ($kg\ h^{-1}\ w^{-1}$)	Power input to refrigerant by compressor (W)	Refrigerant COP	Evaporaing temperature (°C)
450	2025	421	0.10	934	7.25	3.1
350	1574	434	0.11	617	8.24	3.5
250	1189	441	0.12	410	9.21	4.4
150	760	462	0.13	199	11.56	5.6

[a]Tank-water temperature = 6.7°C.

Table A.3. Variable plate-loading test results for unit one

COP	Condenser heat output (W)	Evaporator load (W)	Plate loading (W/m^2)	Evaporating temperature (°)	No. of active plates
3.08	5896	4905	1397	−3.4	4
2.99	5490	4519	1716	−4.6	3
2.70	4824	4068	2318	−6.4	2
2.05	3251	953	2759	−10.5	1

Source: V. D. Baxter, *Intermediate Report on the Performance of Plate-Type Ice-Maker Heat Pumps*, ORNL/CON-23 (October 1978).

Table A.4. Water-chilling performance of units one and four

Tank temperature (°C)	Evaporating temperature (°)	Heating capacity (W)	Plate loading (W/m^2)	Compressor power (w)	COP
		Unit one[a]			
8.2	4.2	8417	1954	2075	4.06
6.5	3.1	7953	1828	2047	3.89
5.0	1.7	7547	1720	2012	3.75
3.8	−0.2	7253	1642	1984	3.65
3.0	−0.7	7082	1598	1965	3.60
		Unit four			
6.7	3.8	7887	1886	2060	3.83
5.7	2.7	7819	1804	2051	3.81
3.9	1.6	7068	1599	1999	3.54
3.2	0.8	7059	1561	1993	3.49
3.1	0.0	6964	1533	1967	3.54

[a]Data excerpted from V. D. Baxter, *Intermediate Report on the Performance of Plate-Type Ice-Maker Heat Pumps*, ORNL/CON-23 (October 1978).

Table A.5. Water-chilling performance of units two and three

Tank temperature (°C)	Suction pressure (kPa)	Heating capacity (W)	Plate loading (W/m^2)	Compressor power (W)	COP
		Unit two[a]			
8.2	400	10,876	3,000	2,849	3.82
6.5	379	10,294	2,794	2,786	3.70
5.0	366	9,712	2,601	2,736	3.55
3.8	352	9,402	2,504	2,691	3.49
3.0	331	9,026	2,382	2,650	3.41
		Unit three			
11.9	441	12,023	1,709	3,099	3.88
9.4	407	11,068	1,590	2,983	3.71
7.3	386	10,396	1,410	2,912	3.57
5.1	352	9,389	1,281	2,878	3.29
3.5	331	9,002	1,158	2,744	3.28
2.1	310	8,423	1,104	2,592	3.25

[a]Data excerpted from V. D. Baxter, *Intermediate Report on the Performance of Plate-Type Ice-Maker Heat Pumps*, ORNL/CON-23 (October 1978).

Table A.6. Performance of test units in freeze-harvest cycle mode for various freeze cycle lengths

Freeze time (min)	Heating capacity (W)	Plate loading (W/m^2)	Compressor power (W)	COP	Harvest-pump power (W)	Compressor and harvest-pump COP
			Unit one, original hot gas			
10	4331	817	1951	2.22		
20	5142	1047	1955	2.63		
30	5321	1104	1921	2.77		
40	5506	1161	1912	2.88		
60	5651	1208	1877	3.01		
70	5750	1236	1879	3.06		
			Unit one, modified hot gas			
10	4693	1135	1713	2.74		
20	5233	1195	1766	2.96		
35	5425	1211	1783	3.04		
70	5341	1199	1744	3.06		
			Unit four			
10	6016	1599	1928	3.12		
30	5834	1356	1870	3.12		
60	5806	1318	1840	3.16		
90	5616	1287	1823	3.08		
			Unit two[a]			
5	7702	1908	2647	2.91		
11	7732	1918	2648	2.92		
15	7455	1836	2597	2.87		
20.5	7323	1823	2491	2.94		
			Unit three			
15	8237	1255	2636	3.13	124	3.11
30	7881	1161	2601	3.03	125	3.02
45	7807	1113	2594	3.01	125	3.00
60	7666	1091	2570	2.98	123	2.98
75	7364	1019	2471	2.98	124	2.97
			Unit three[b]			
15	8172	1285	2649	3.09	138	3.04
30	7746	1191	2604	2.97	137	2.95
60	7423	1102	2527	2.94	138	2.93

[a]Data excerpted from *V. D. Baxter, Intermediate Report on the Performance of Plate-Type Ice-Maker Heat Pumps,* ORNL/CON-23 (October 1978).

[b]Air temperature around plates lowered to 1.7°C.

Table A.7. Performance of test units under steady freeze (no-harvest) conditions

Freeze time (min)	Heating capacity (W)	Plate loading (W/m^2)	Evaporator loading (W)	Compressor power (W)	COP	Suction pressure (kPa)
			Unit one			
5	6193	1574	5528	1859	3.33	331
20	6043	1391	4882	1847	3.27	328
35	5782	1309	4596	1822	3.17	317
50	5656	1281	4499	1803	3.14	312
65	5573	1268	4451	1789	3.12	305
80	5504	1255	4412	1780	3.09	300
95	5444	1246	4378	1772	3.07	299
110	5386	1240	4353	1765	3.05	295
125	5315	1230	4316	1760	3.02	292
			Unit two			
5	7615	1962	5465	2389	3.19	317
20	6855	1725	4806	2277	3.01	290
35	6538	1624	4527	2235	2.93	285
50	6273	1539	4294	2199	2.86	271
65	6077	1479	4120	2174	2.79	263
80	5953	1438	4005	2164	2.75	257
95	5843	1397	3897	2163	2.70	255
110	5761	1366	3809	2168	2.65	261
125	5721	1347	3750	2190	2.61	247
			Unit three			
5	8963	1391	7761	2737	3.27	297
20	8402	1296	7224	2706	3.11	300
35	7822	1164	6496	2616	2.99	274
50	7381	1088	6064	2563	2.88	271
65	7133	1044	5826	2530	2.82	268
80	6964	1009	5620	2507	2.78	261
95	6835	984	5485	2483	2.75	255
110	6727	965	5378	2468	2.73	248
125	6627	949	5287	2452	2.70	245
			Unit four[a]			
5	5576			1963	2.84	317
20	5888	1580	5549	1931	3.05	321
35	5857	1523	5343	1902	3.08	312
50	5801	1479	5196	1890	3.07	310
65	5738	1445	5069	1875	3.06	305
80	5676	1416	4976	1861	3.05	300
95	5602	1391	4878	1849	3.03	297
110	5669	1400	4911	1841	3.08	295
125	5482	1350	4738	1833	2.99	291

[a]Ambient air temperature = 5.6°C.

APPENDIX B

SAMPLE CALCULATIONS

SAMPLE TEST

A sample test for unit three consisted of a 45-min freeze time with 2-min harvest; test duration was two complete cycles.

A. Data

Table B.1 shows a sample output from the laboratory data acquisition system containing temperature and power consumption data taken at 1-min intervals. Pressure data were manually recorded from gauges. Temperatures and power consumption are illustrated in Figs. B.1 and B.2.

Table B.1. Sample data output for 45-min freeze-cycle test on unit three for period of operation immediately preceding, during, and immediately following an ice-harvesting operation

Temperature[a] and power consumption[b]	Scan									
	43	44	45	46	47	48	49	50	51	52
T_1	220.35	220.16	220.96	220.80	205.68	185.41	211.35	215.43	214.98	214.60
T_2	101.80	102.36	101.57	101.59	100.22	94.48	101.80	103.16	103.72	103.90
T_3	85.68	86.06	86.15	86.40	85.86	85.23	67.65	68.58	70.37	71.58
T_4	80.32	80.49	80.56	80.65	80.60	80.89	69.14	65.83	66.66	67.87
T_5	19.83	21.30	19.99	21.65	32.06	34.04	26.80	24.50	31.55	34.52
T_6	46.48	46.04	46.07	45.49	53.34	64.43	53.92	48.28	46.70	46.58
T_7	61.87	61.94	62.03	62.22	82.20	78.23	73.66	71.66	70.26	69.25
T_8	55.60	55.67	55.68	55.79	42.43	43.78	44.90	46.26	47.46	48.46
T_9	83.78	84.04	84.33	84.64	84.97	85.15	84.38	84.28	84.12	83.91
T_{10}	83.66	83.88	84.16	84.43	71.31	60.24	57.36	58.86	59.96	60.72
T_{11}	116.55	116.36	116.56	116.27	115.41	114.06	115.22	116.03	116.70	116.88
T_{12}	59.88	59.91	59.96	59.96	60.02	60.44	60.78	60.07	59.92	59.86
P_C	2499.20	2524.80	2443.10	2401.20	15.10	16.10	2578.00	2640.70	2665.10	2665.20
P_{HP}	0.24	0.02	0.04	0.02	124.94	124.92	0.20	0.00	0.02	0.08

[a]Temperature given in degrees Fahrenheit.
[b]Power consumption given in watts.

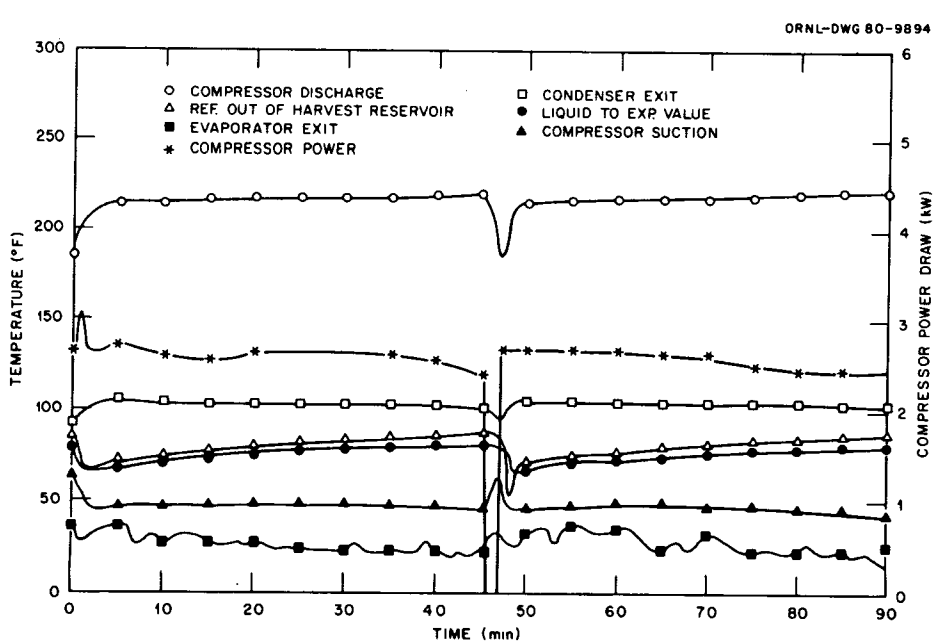

Fig. B.1. Sample test data, refrigerant temperatures, and compressor power vs time.

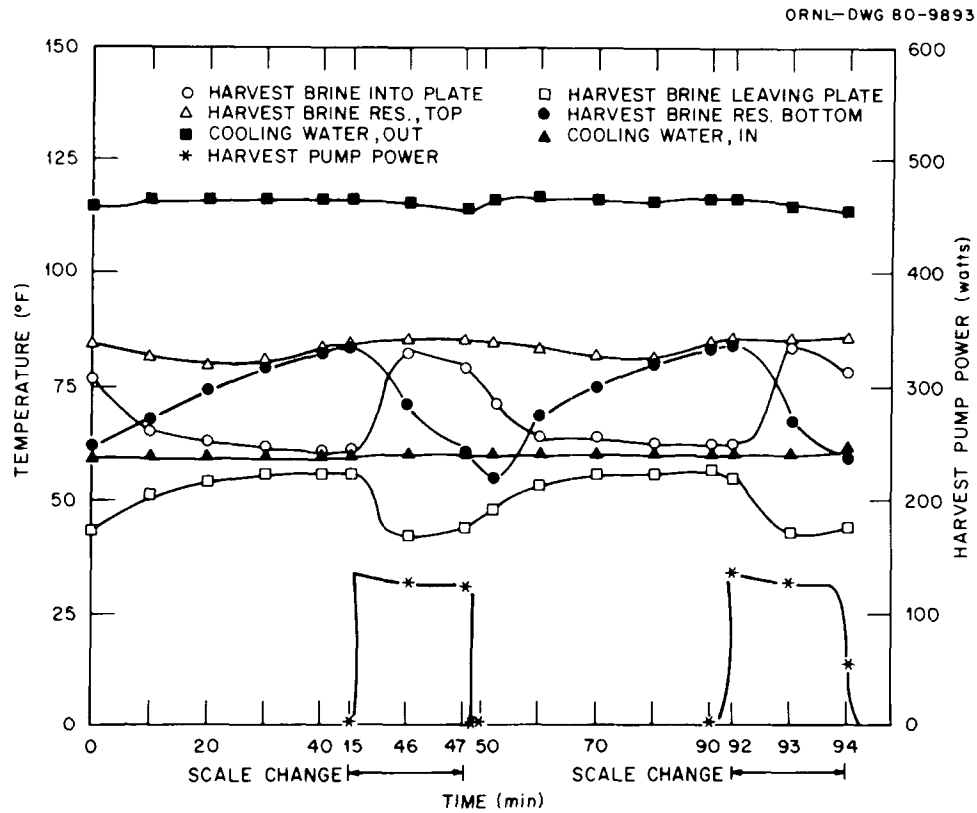

Fig. B.2. Sample test data, brine and coolant temperatures, and harvesting pump power vs time.

Compressor power and refrigerant temperatures were averaged over the compressor run time; harvest-pump power and harvest-brine inlet and outlet temperatures were averaged over the harvesting period. These averages, along with the total coolant-water flow and average refrigerant pressures, are listed below.

1. Compressor discharge: T_1 = 217.0°F (102.8°C), P_1 = 221 psig (1524 kPa)
2. Condenser exit: T_2 = 103.1°F (39.5°C), P_2 = 216 psig (1489 kPa)
3. Refrigerant out of harvest brine reservoir: T_3 = 79.3°F (26.3°C)
4. Liquid to expansion valve: T_4 = 75.0°F (23.9°C)
5. Evaporator exit: T_5 = 26.1°F (−3.3°C), P_5 = 45 psig (310 kPa)
6. Compressor suction: T_6 = 47.2°F (8.4°C), P_6 = 42 psig (290 kPa)
7. Harvest brine into plates: T_7 = 80.1°F (26.7°C)
8. Harvest brine out of plates: T_8 = 42.9°F (6.1°C)
9. Harvest-brine reservoir, top: T_9 = 82.2°F (27.9°C)
10. Harvest-brine reservoir, bottom: T_{10} = 74.0°F (23.3°C)
11. Cooling water out: T_{11} = 116.6°F (47.0°C)
12. Cooling water in: T_{12} = 59.9°F (15.5°C)
13. Compressor power draw: P_C = 2596.8 W
14. Harvest-pump power draw: P_{HP} = 124.7 W
15. Total cooling water used: W_C = 84.6 gal (320 L)
16. Compressor run time: θ_C = 1.5 h

17. Harvesting-pump run time: $\theta_{HP} = 0.067$ h
18. Average evaporator inlet pressure: $P_{EI} = 52$ psig (359 kPa)
19. Harvest-brine flow rate: $\dot{m}_B = 33.8$ lb/min (0.26 kg/s)

B. Calculations

1. Heating capacity: $Q_H = [8.33(W_C/\theta_C)]\,(T_{11} - T_{12})$; assumes $c_p = 1$ Btu/lb·°F for cooling water

$$Q_H = \frac{(8.33)(84.6)(116.6 - 59.9)}{1.5}$$

$$= 26{,}638 \text{ Btuh } (7807 \text{ W})$$

2. Evaporator load: $Q_E = \dot{m}_R(h_5 - h_4)$, where

$\dot{m}_R$ = refrigerant flow rate

$$= \frac{Q_H}{(h_1 - h_2)}$$

h_n = refrigerant enthalpy at point n, Btu/lb[a] (kJ/kg)

$$\dot{m}_R = \frac{26638}{136.3 - 40.2}$$

$$= 280.1 \text{ lb/h } (0.35 \text{ kg/s})$$

$$Q_E = 280.1(107.2 - 31.6)$$

$$= 21176 \text{ Btuh } (6206 \text{ W})$$

3. Plate loading: $\bar{Q}_E = Q_E/A_E$, where

A_E = active evaporator area, 60 ft^2 (5.57 m^2)

$\bar{Q}_E = 21{,}176/60 = 353$ Btuh/ft^2 (1113 W/m^2)

4. Compressor-only COP: COP = Q_H/P_C

$$\text{COP} = \frac{26{,}638}{2596.8 \times 3.412}$$

$$= 3.01$$

5. Compressor and harvesting pump COP: COP = $Q_H\theta_C/P_C\theta_C + P_{HP}\theta_{HP}$

$$\text{COP} = \frac{(26{,}638)(1.5)}{[(2596.8)(1.5) + (124.7)(0.0067)] \times 3.412}$$

$$= 3.00$$

6. Power input to refrigerant by compressor: $P_c' = \dot{m}_R(h_1 - h_6)$

$$P_c' = 280.1(135.3 - 111.0)/3.412$$

$$= 1995 \text{ W}$$

[a]Obtained from ASHRAE R-22 property tables.

7. Refrigerant COP: $COP' = Q_H / P_c'$

$$COP' = \frac{26638}{1996 \times 3.412}$$

$$= 3.91$$

CYCLIC-TEST SAMPLE CALCULATIONS

Test unit three, 80% on time, 12-min compressor run time, 4 cph.

A. Data

Test duration: $\theta = 1.0$ h
Compressor run time: $\theta = 0.8$ h
Compressor draw: $P_C = 2671.4$ W
Total coolant flow: $W_C = 55.55$ gal (210.3 L)
Cooling water out: $T_o = 113.1°F$ (45.1°C)
Cooling water in: $T_i = 65.6°F$ (18.7°C)
Harvest-pump draw: $P_H = 132.8$ W
Harvest-pump run time: $\theta_H = 0.133$ h

B. Calculations

1. Cyclic heating output, Q_{o_C}

$$Q_{o_C} = (8.33W_C)[c_p(T_o - T_i)]$$

$$= 8.33(55.55)(1)(113.1 - 65.6)$$

$$= 21{,}980 \text{ Btu } (6443 \text{ Wh})$$

2. Part load factor, PLF

$PLF = Q_{o_C} / \dot{Q}_{o_{ss}}\theta$, where

$\dot{Q}_{o_{ss}}$ = steady-state full-load output for a 1-h freeze cycle[a]

$\dot{Q}_{o_{ss}} = 25{,}328$ Btu/h (7423 W)

$COP_{ss} = 2.93$

Thus,

$$PLF = \frac{21{,}980}{25{,}328 \times 1}$$

$$= 0.87$$

[a]From Table A.6, for a 60-min freeze time and 1.7°C air around the evaporator plates.

3. Cyclic COP

$$COP_c = \frac{Q_o}{P_C\theta_C + P_H\theta_H}$$

$$= \frac{21{,}980}{(2671.4 \times 0.8) + (132.8 \times 0.133)}$$

$$= 2.99$$

4. $COP_c/COP_{ss} = 2.99/2.93 = 1.02$

The cyclic COP is higher because of the reasons outlined in Sect 5.3.2. Cyclic-test freeze time was only 12 min, compared with 1 h for the baseline test; therefore, thinner ice was made, and evaporating temperature did not fall as much.

SAMPLE CALCULATIONS FOR BUCKET AND BULK ICE-PACKING FACTOR TESTS

A. Bucket-sampling test (sample 3, Table 4)

1. Apparent packing factor, PF_w'

$W_{t\ \mathrm{ice}} = 3.42$ kg

$W_{t\ \mathrm{ice+water}} = 7.00$ kg

$PF_w' = 3.42/7.00 = 0.49$

2. Calorimeter test data

W_{ice} = ice sample weight = 0.58 kg

W_{H_2O} = water weight = 2.5 kg

T_{ice} = ice sample temperature = 32°F (0°C)

T_{H_2O} = water temperature = 101.2°F (38.4°C)

T_M = mixture temperature = 64.4°F (18.0°C)

Results: ΔU(ice sample) = ΔU(water)

$W_{si}h_{fi} + W_{\mathrm{ice}}(T_M - T_{\mathrm{ice}}) = W_{H_2O}(T_{H_2O} - T_M)$, where

W_{si} = weight of solid ice in ice sample

h_{fi} = heat of fusion of ice, 144 Btu/lb

Solving for W_{si}:

$$W_{si} = \frac{W_{H_2O}(T_{H_2O} - T_M) - W_{\mathrm{ice}}(T_M - T_{\mathrm{ice}})}{h_{fi}}$$

$$= \frac{2.5(101.2 - 64.4) - 0.58(64.4 - 32)}{144}$$

$$= 0.508 \text{ kg}$$

$SF = 0.508/0.58 = 0.876$

3. Actual packing factor, PF

$$PF_w = PF'_w SF$$

$$= 0.49 \times 0.876$$

$$= 0.43$$

$$PF = \frac{PF_W}{0.917 + PF_W \times 0.083}$$

$$= 0.43/0.95$$

$$= 0.45$$

B. Bulk-sampling test (sample 2, Table 5)

1. Data: Figure B.3, a cross section of the ice bin for test unit two, illustrates the following measurements taken during the bulk testing.

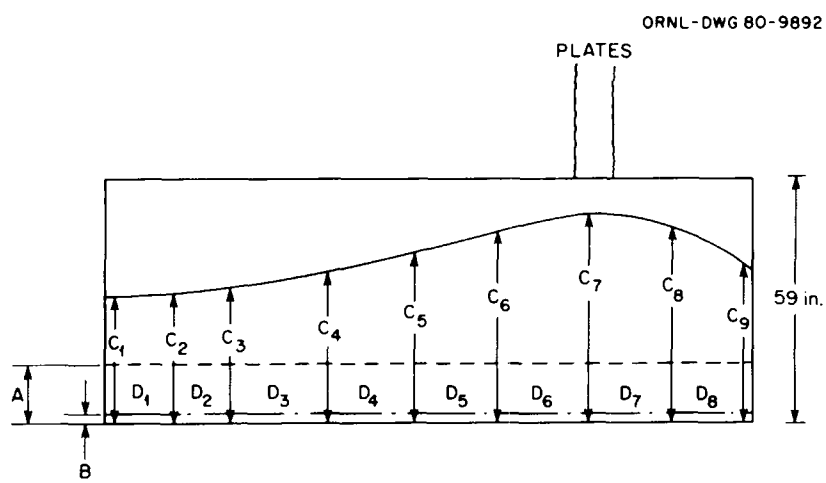

Fig. B.3. Cross section of unit two ice tank; measurements taken during bulk-sampling tests are shown.

A = initial water level, 14 in. (0.36 m)

B = final water level, 3.25 in. (0.08 m)

C_x = ice-pack thickness (at various points), in. (m)

D_x = distance between points C, in. (m)

C_1 = 12 (0.30)	D_1 = 12 (0.30)
C_2 = 16.5 (0.42)	D_2 = 12 (0.30)
C_3 = 21.25 (0.54)	D_3 = 12 (0.30)
C_4 = 27.0 (0.69)	D_4 = 12 (0.30)
C_5 = 32.75 (0.83)	D_5 = 12 (0.30)
C_6 = 36.125 (0.92)	D_6 = 14 (0.36)
C_7 = 40.5 (1.03)	D_7 = 8 (0.20)
C_8 = 38.125 (0.97)	D_8 = 21 (0.53)
C_9 = 32.75 (0.83)	

Tank dimensions: 103 in. (2.62 m) long, 48 in. (1.22 m) wide, 59 in. (1.50) m) deep

2. Calculations:

a. Ice volume, V_I

$V_I = A_{cs} \times$ tank width, where

A_{cs} = ice cross-sectional area, $A_1 + A_2 + \cdots + A_8$, assuming each section to be a trapezoid: $A_x = 0.5(C_x + C_{x\times1})D_x$

$V_I = (3054 \text{ in.}^2)(48 \text{ in.})(1 \text{ ft}^3/1728 \text{ in.}^3)$

$= 84.83 \text{ ft}^3 \ (2.40 \text{ m}^3)$

b. Weight of water converted into ice, W_I

$W_I =$ tank length $\times$ tank width $\times [A - (1 - PF)B] \times 62.4 \text{ lb/ft}^3$

The ice on the bottom is assumed to be compacted and thus to have a packing factor of 0.6 (Table 4)

$W_I = 103 \times 48 \times [12 - 0.4(3.25)] \times 1 \text{ ft}^3/1728 \text{ in.}^3 \times 62.4$

$= 2267.5 \text{ lb} \ (1028.5 \text{ kg})$

c. Rectangular bin volume required to hold ice, V_B

$V_B =$ length $\times$ width $\times C_7$

$= (103)(48)(40.5)(1/1728)$

$= 115.9 \text{ ft}^3 \ (3.28 \text{ m}^3)$

d. Bin volume packing factor, PF_B

$$PF_B = \frac{W_I}{V_B \times 57.24}$$

$$= \frac{2267.5}{115.9 \times 57.24}$$

$= 0.34$

e. Ice-volume packing factor, PF_I

$$PF_I = \frac{W_I}{V_I \times 57.24}$$

$$= \frac{2267.5}{84.83 \times 57.24}$$

$= 0.47$

f. Original water volume, V_w

$V_w =$ length $\times$ width $\times A$

$= (103)(48)(14)(1/1728)$

$= 40.1 \text{ ft}^3 \ (1.13 \text{ m}^3)$

APPENDIX C

RELATIONSHIP BETWEEN THE PACKING FACTOR AND THE WEIGHT-FRACTION PACKING FACTOR

The packing factor has been defined as

$$PF = V_I / V_T \equiv \frac{\text{ice volume}}{\text{total wetted volume at full ice}},$$

which can also be expressed as

$$PF = W_I / \rho_I V_T ,$$

where

W_I = ice weight,

ρ_I = ice density at 0°C = 0.917 g/cm^3 (57.24 lb/ft^2).

The weight-fraction packing factor has been defined as

$$PF_w = W_I / W_T ,$$

where

$W_I \equiv$ ice weight,

$W_T \equiv$ total ice and water weight.

This can also be expressed as

$$PF_w = V_I \rho_I / V_i \rho_w ,$$

where

$V_i \equiv$ water volume at no ice,

$\rho_w \equiv$ water density at 0°C = 1.0 g/cm^3 (62.4 lb/ft^3).

But also,

$$V_i = V_I \rho_I / \rho_W + (V_T - V_I)$$

or

$$V_i = V_T PF \left(\frac{\rho_I}{\rho_W}\right) + V_T(1 - PF)$$

$$= V_T \left[1 + PF \left(\frac{\rho_I}{\rho_w} - 1\right)\right].$$

Therefore,

$$PF_w = \frac{V_I \rho_I}{V_T \rho_w \left[1 + PF \left(\frac{\rho_I}{\rho_w} - 1\right)\right]}.$$

Collecting terms and solving for PF,

$$PF_w = \frac{PF_w}{\frac{\rho_I}{\rho_W} + PF_w\left(\frac{\rho_I}{\rho_W} - 1\right)} .$$

Substituting for ρ_I and ρ_w yields

$$PF = \frac{PF_w}{0.917 + 0.083\ PF_w} .$$

INTERNAL DISTRIBUTION

1. L. A. Abbatiello
2. H. G. Arnold
3. V. D. Baxter
4. J. L. Bledsoe
5. V. R. Brantley
6. R. S. Carlsmith
7. F. C. Chen
8. W. L. Cooper, Jr.
9. F. A. Creswick
10. G. A. Cristy
11. J. G. Delene
12. J. R. DeMonbrun
13. R. C. DeVault
14. M. D. Eden
15. S. K. Fischer
16. R. J. Friar
17. W. Fulkerson
18. R. E. Gant
19. V. O. Haynes
20. E. C. Hise
21. H. W. Hoffman
22. R. B. Honea
23. W. L. Jackson
24. G. E. Kamp
25. C. G. Lawson
26. W. P. Levins
27. H. M. Long
28. V. C. Mei
29. J. W. Michel
30. D. R. Miller
31. R. E. Minturn
32. W. R. Mixon
33. J. C. Moyers
34. E. A. Nephew
35. H. Perez Blanco
36. G. D. Pine
37. G. T. Privon
38. D. T. Rizy
39. R. C. Robertson
40. M. W. Rosenthal
41. J. W. Sims
42. L. H. Thomas
43. D. P. Vogt
44. D. J. Walukas
45. T. J. Wilbanks
46. Biology Division Library
47–48. Central Research Library
49. Document Reference Section
50. Emergency Technology Library
51–52. Energy Information Library
53. Laboratory Records RC
54–56. Laboratory Records Department
57. ORNL Patent Section

EXTERNAL DISTRIBUTION

58. Roy W. Abbott, Manager, Advanced Technology, General Electric Company, Appliance Park, Building 6-208, Louisville, KY 40225
59. Ben Adams, Adams Craft Herz Walker, 106 Administration Road, Oak Ridge, TN 37830
60. Kent Anderson, Trane Company, 2020 14th Street, Arlington, VA 22201
61. Bruce Appelbaum, Gordian Associates, Inc., 711 Third Avenue, New York, NY 10017
62. Arthur G. Baitz, Assistant Vice President and Director of Planning, Robertshaw Controls Company, 1701 Byrd Avenue, P.O. Box 26544, Richmond, VA 23261
63. Hamp Barnett, Power Research Staff, Tennessee Valley Authority, 350 Commerce Union Bank Building, Chattanooga, TN 37401
64. Larry B. Barrett, Potomac Electric Power Company, Manager, Energy Management Services Division, 1900 Pennsylvania Avenue NW, Washington, DC 20068
65. John Blair, 1019 Bellemeade, Evansville, IN 47714
66. Thomas P. Bligh, Department of Mechanical Engineering, University of Minnesota, Minneapolis, MN 55455
67. Robert L. Boyd, 413 Brewers Creek Lane, Carrollton, VA 23314
68. Gene Brewer, NIBS, Suite 700, 1015 15th Street NW, Washington, DC 20005
69. William B. Briggs, McDonnell-Douglas Company, Department EO8O, P.O. Box 516, St. Louis, MO 63166

70. Thomas Cahill, Energy Systems Division, Carrier Corporation, Carrier Tower, Post Office Box 4800, Syracuse, NY 13221
71. James M. Calm, Argonne National Laboratory, Energy & Environmental Systems Division, Building EES-11, Argonne, IL 60439
72. Joe Canal, General Electric Company, Troup Highway, Tyler, TX 75711
73. Louis-Marie Chounet, Batiment 200, Lab de l'Accelerateur Lineaire, 91405 Orsay, France
74. W. James Cole, Program Director, New York State Energy Research and Development Authority, Agency Building No. 2, Empire State Plaza, Albany, NY 12223
75. David Colvin, Triangle Research and Development Corporation, P.O. Box 12696, Research Triangle Park, NC 27709
76. Ronald Cosby, Department of Physics and Astronomy, Ball State University, Muncie, IN 47306
77. George E. Courville, Department of Physics, Fairleigh-Dickinson University, Teaneck, NJ 07666
78. John J. Cuttica, Chief, Technology and Consumer Products Branch, Mail Stop GH-068, Department of Energy, 1000 Independence Avenue SW, Washington, DC 20585
79. H. E. Davis, Concentration Specialists, Inc., 26 Dundee Park, Andover, MA 01810
80. Charles E. Dorgan, University of Wisconsin (Extension), 432 North Lake Street, Madison, WI 53701
81. Gordon D. Duffy, Executive Editor, Air Conditioning News, 700 East Maple, Birmingham, MI 48011
82. William A. Elder, President, Automated Air Systems, Inc., 1723 Rhoadmiller Street, Richmond, VA 23220
83. Harry C. Fischer, P.O. Box 1687, Cocoa, FL 32922
84. Douglas Funkhouser, Urban Systems Research and Engineering, Inc., 36 Boylston Street, Cambridge, MA 02138
85. Don P. Gatley, Gatley & Associates, 489 Westover Drive, NW, Atlanta, GA 30305
86. Ted Gillis, Lennox Industries, Promenade Towers, P.O. Box 400450, Dallas, TX 75240
87. George E. Gilmore, Consolidated Edison Company of New York, Inc., Four Irving Place, New York, NY 10003
88. L. R. Glicksman, Department of Mechanical Engineering, Massachusetts Institute of Technology, Cambridge, MA 02139
89. David Goldenberg, TRW Energy Systems Inc., 800 Oak Ridge Turnpike, Oak Ridge, TN 37830
90. Dieter Grether, Vice President, Engineering, Friedrich Air Conditioning and Refrigeration, P.O. Box 1540, San Antonio, TX 78295
91. Gerald C. Groff, Research Division, Carrier Corporation, Syracuse, NY 13201
92. Donald G. Hoffard, P.O. Box 3221, N. E. Holladay, Portland, OR 97208
93. F. Honnold, Consumer Products Division, Carrier Corporation, Syracuse, NY 13201
94. E. J. Horan, Exxon Research and Engineering Company, P.O. Box 8, Linden, NJ 07036
95. H. Jaster, General Electric Corporate Research and Development, General Electric Company, Schenectady, NY 12301
96. Larry L. Jenkins, Jenkins, Mack & Associates Inc., 2205 North 91st Court, Omaha, NB 68134
97. Ralph F. Jones, Brookhaven National Laboratory, Upton, Long Island, NY 11973
98. Ted Kapus, Director, Consumer Products Division, Mail Stop GH-086, Department of Energy, 1000 Independence Avenue SW, Washington, DC 20585
99. Richard M. Kelso, Associate Professor, School of Architecture, University of Tennessee, 100 Estabrook Hall, Knoxville, TN 37916
100. R. W. King, Manager, Advanced Engineering, Copeland Corporation, Sydney, OH 45365
101. William A. Knox, 111 Edgewood Avenue, Columbia, MO 65201
102. William Kolosi, Ohio Edison Company, 76 South Main, Akron, OH 44308
103. Sherman Kouns, Sales Representative, General Shale Products Corporation, P.O. Box 733, Knoxville, TN 37901

104. Edward A. Kush, Associate Scientist, Solar Research Group, Brookhaven National Laboratory, Upton, NY 11973
105. Jim Leggoe, Philadelphia Electric Company, 2301 Market Street, Philadelphia, PA 19101
106. Herbert Lindahl, Manager, Advanced Engineering, Bohn Aluminum and Brass Corporation, Heat Transfer Division, 1625 East Voorhees Street, Danville, IL 61832
107. Quentin Looney, Energy Utilization and Conservation Technology, Electric Power Research Institute, 3412 Hillview Avenue, P.O. Box 10412, Palo Alto, CA 94303
108. Harold G. Lorsch, Manager, Energy Laboratory Engineering Department, The Franklin Institute Research Laboratories, Twentieth and Parkway, Philadelphia, PA 19103
109. Hubert P. Luckett, Editor-in-Chief, *Popular Science,* 380 Madison Avenue, New York, NY 10017
110. I. Ward MacArthur, Honeywell, Inc., 2600 Ridgway Parkway, NE, Minneapolis, MN 55413
111. Calvin D. MacCracken, Calmac Manufacturing Company, 150 South Van Brunt Street, Englewood, NJ 07631
112. Merle McBride, Owens-Corning Technical Center, Route 16, P.O. Box 415, Granville, OH 43023
113. Jim McCallum, Executive Editor, Air Conditioning and Refrigeration Business, 614 Superior Avenue West, Cleveland, OH 44113
114. Jack McCormick, Research Engineer, Northern States Power Company, 414 Nicollet Mall, Minneapolis, MN 55401
115. Robert Mauro, Electric Power Research Institute, 3412 Hillview Avenue, P.O. Box 10412, Palo Alto, CA 94303
116. John Millhone, Director, Office of Buildings and Community Systems, Mail Stop GH-068, Department of Energy, 1000 Independence Avenue SW, Washington, DC 20585
117. Dan Myers, Refrigeration Systems, 4241 Hogue Rd, Evansville, IN 47712
118. Kenneth J. Nemeth, Executive Director, Southern States Energy Board, 2300 Peachford Road, One Exchange Place, Suite 1230, Atlanta, GA 30338
119. J. A. O'Brien, Director, Bedford Administrative Operation, The Mitre Corporation, Bedford, MA 01730
120. Bill Riley, Chief Engineer, Advance Development, Heil-Quaker Corporation, 647 Thompson Lane, P.O. Box 40566, Nashville, TN 37204
121. James K. Risher, Energy Resources Center, Honeywell, Inc., 2600 Ridgway Parkway, Minneapolis, MN 55413
122. A. H. Rosenfeld, Lawrence Berkeley Laboratory, Building 50B, Room 5246, Berkeley, CA 94720
123. David P. Ross, Senior Scientist, Energy Resources and Conservation Division, Science Applications, Inc., 2028 Powers Ferry Road, Suite 260, Atlanta, GA 30339
124. John D. Ryan, Program Manager, Technology and Consumer Products Branch, Mail Stop GH-068, Department of Energy, 1000 Independence Avenue, SW, Washington, DC 20585
125. James L. Schulze, Technology Program Manager, General Electric Company, Appliance Park, Louisville, KY 40225
126. Charles F. Sepsy, The Ohio State University Department of Mechanical Engineering, 206 W. 18th Avenue, Columbus, OH 43210
127. Charles Shattenkirk, Box 82H, RD2, Valatie, NY 12184
128. Mason H. Somerville, Manager, Engineering Experiment Station, University of North Dakota, Grand Forks, ND 58202
129. E. Spannhake, White Consolidated Industries, 11770 Berea Road, Cleveland, OH 44111
130. Richard D. Stewart, Manager, Advanced Technology Programs, General Electric Company, Appliance Park, Building 35, Louisville, KY 40225
131. Steven Strong, Solar Design Associates, 271 Washington Street, Canton, MA 02021
132. Floyd Stuckey, FSA Engineering Consultants, 315 East Sixth Street, Winfield, KS 67156
133. Waler D. Syniuta, Advanced Mechanical Technology Inc., 141 California Street, Newton, MA 02158

134. Robert T. Tamblyn, Engineering Interface Limited, 1200 Sheppard Avenue East, Toronto, Ontario M2K2R8
135. Susan S. Waddle, Department of Energy, Oak Ridge Operations Office, Oak Ridge, TN 37830
136. Frank S. Wang, Research Specialist, Functional Products and Systems, Larkin Lab, Swede Road, Midland, MI 48640
137. H. F. Waser, FHP Manufacturing Company, 610 Southwest 12th Avenue, Pompano Beach, FL 33060
138. Robert G. Werden, Werden & Associates, Inc., P.O. Box 414, Jenkintown, PA 19046
139. Frank White, AiResearch Manufacturing Company, P.O. Box 3413, Oak Ridge, TN 37830
140. Kyle E. Wilcutt, South Co. Services, P.O. Box 720071, Atlanta, GA 30346
141. M. Wilden, University of New Mexico, Albuquerque, NM 87115
142. David J. Young, Ontario Hydro Research, 800 Kipling Avenue, Toronto, Ontario, Canada M8Z 5S4
143. Institute of Energy Analysis, ORAU Library, Oak Ridge, TN 37830
144. Assistant Manager, Energy Research & Development, DOE-ORO, Oak Ridge, TN 37830

145 171. Technical Information Center, Department of Energy, P.O. Box 62, Oak Ridge, TN 37830

172 626. External Energy Conservation Distribution Mailing List and Energy Conservation Office (9102-1, Rm 2)

☆U.S. GOVERNMENT PRINTING OFFICE: 1980-640-245/279